CHARACTERIZATION OF OXYGEN-INDEPENDENT FUNCTIONS OF MYOGLOBIN IN MITOCHONDRIAL REGULATION

by

Janelle Lynn Bickta

Bachelor of Science in Bioengineering, University of Pittsburgh, 2013

Submitted to the Graduate Faculty of

Swanson School of Engineering in partial fulfillment

of the requirements for the degree of

Master of Science

University of Pittsburgh

2015

UNIVERSITY OF PITTSBURGH

SWANSON SCHOOL OF ENGINEERING

This thesis was presented

by

Janelle Bickta

It was defended on

March 18, 2015

and approved by

Sanjeev Shroff, PhD, Distinguished Professor and Chair, Department of Bioengineering

Michael Lotze, MD, Professor and Vice Chair of Research, Department of Surgery

Adam Straub, PhD, Assistant Professor, Department of Pharmacology and Chemical Biology

Thesis Advisor: Sruti Shiva, PhD, Associate Professor, Department of Pharmacology and Chemical Biology

CHARACTERIZATION OF OXYGEN-INDEPENDENT FUNCTIONS OF MYOGLOBIN IN MITOCHONDRIAL REGULATION

Janelle Bickta, M.S.

University of Pittsburgh, 2015

Myoglobin and mitochondria have been studied extensively over the past century; however, the mechanisms by which they interact still remain unclear. Myoglobin is known for its localization in skeletal muscle where it stores and transports oxygen to respiring mitochondria. Myoglobin is now gaining recognition for its expression in cancer and its function as a nitrite reductase, able to reduce nitrite to nitric oxide (NO). The overall objective of this study is to characterize the regulation of mitochondria by myoglobin, specifically in ischemia/reperfusion injury and breast cancer.

Mitochondrial damage is a central component to ischemia/reperfusion injury. Nitrite is known to mediate protection after ischemia/reperfusion through its reduction to NO, which S-nitrosates complex I of the electron transport chain. This S-nitrosation reduces reactive oxygen species generation, thereby reducing cell death. Using myoglobin positive and negative cells, this study shows that nitrite is only able to mediate protection in myoglobin-expressing cells through S-nitrosation. Furthermore, by knocking down complex I by siRNA transfection, it is confirmed

that this protection occurs through complex I. Therefore, myoglobin expression is required for nitrite to have protective effects in reperfusion injury.

Myoglobin has only recently been discovered in cancer tumors; therefore, little is known about its function in these tissues. Interestingly, myoglobin expression in breast cancer has been associated with better patient prognosis. In this study, stable transfection of myoglobin in MDA-MB-231 breast cancer cells caused a significant decrease in cell proliferation and marked mitochondrial fusion. This fusion of mitochondria resulted in cell cycle arrest at the G1/S phase transition of the cell cycle. Further investigation showed that myoglobin expression prevents ubiquitination of mitochondrial fusion proteins. Myoglobin-expressing cells therefore have extensive mitochondrial fusion, which causes cell cycle arrest and reduced cell proliferation and tumor growth *in vivo.*

This project has identified that myoglobin is necessary for nitrite to have protective effects in ischemia/reperfusion and begun to elucidate the mechanism by which myoglobin is beneficial in breast cancer. With further research, myoglobin may be used as a therapeutic target for cancer as well as ischemia/reperfusion in other tissues.

TABLE OF CONTENTS

LIST OF FIGURES ..... **X**

NOMENCLATURE ..... **XVI**

PREFACE ..... **XVII**

1.0 INTRODUCTION **1**

1.1 MITOCHONDRIA **1**

1.1.1 Mitochondria are dynamic structures **3**

1.2 MYOGLOBIN **5**

1.2.1 Myoglobin structure and localization **6**

1.3 REGULATION OF MITOCHONDRIA BY MYOGLOBIN **7**

1.3.1 Myoglobin is an oxygen storage protein **7**

1.3.2 Myoglobin-facilitated oxygen diffusion **8**

1.3.3 Myoglobin reacts with reactive nitrogen species to modulate mitochondrial function **9**

1.3.4 Nitric oxide regulates mitochondria **10**

2.0 RESEARCH OBJECTIVES **12**

3.0 EXPERIMENTAL METHODS 13

3.1 REAGENTS 13

3.2 STABLE TRANSFECTION OF MYOGLOBIN IN MDA-MB-231 CELLS 13

3.3 MYOGLOBIN-EXPRESSING CHO CELLS 14

3.4 CELL CULTURE 14

3.5 BRIGHT FIELD IMAGING 15

3.6 S-NITROSATION DETECTION 15

3.7 CHO NDUFAF1 TRANSFECTION 16

3.8 ISCHEMIA/REPERFUSION SIMULATION 16

3.9 LACTATE DEHYDROGENASE ACTIVITY ASSAY 16

3.10 WESTERN BLOT 17

3.11 ^{3}H THYMIDINE INCORPORATION 18

3.12 CRYSTAL VIOLET STAINING 18

3.13 SCRATCH ASSAY 19

3.14 APOPTOSIS MEASUREMENT 19

3.15 FLUORESCENCE IMAGING 19

3.16 TRANSMISSION ELECTRON MICROSCOPY 20

3.17 HYDROGEN PEROXIDE MEASUREMENT 21

3.18 SUPEROXIDE MEASUREMENT 21

3.19 MDA-MB-231 SIRNA TRANSFECTION 22

3.20 MFN1 IMMUNOPRECIPITATION 22

3.21 MEASUREMENT OF PARKIN OXIDATION BY BIOTIN SWITCH 23

3.22 ANIMALS 23

3.23 STATISTICS 24

4.0 RESULTS 25

4.1 AIM 1 25

4.1.1 Stable transfection of human myoglobin in CHO cells 31

4.1.2 Nitrite treatment promotes cell survival after ischemia/reperfusion in CHOMb cells 32

4.1.3 Treating CHOR and CHOMb cells with nitrite increases protein S-nitrosation in CHOMb but not CHOR cells 34

4.1.4 Myoglobin-dependent nitrite-mediated protection occurs through mitochondrial complex I 35

4.2 AIM 2 39

4.2.1 Stable transfection of human myoglobin in MDA-MB-231 cells 40

4.2.2 Myoglobin expression decreases proliferation and migration of MDA-MB-231 cells.. 41

4.2.3 Myoglobin expression does not increase apoptosis 42

4.2.4 Myoglobin expression in 231 cells is associated with mitochondrial fusion 43

4.2.5 Mitochondrial fusion in 231Mb cells is due to upregulation of mfn1 & 2 and downregulation of drp1 45

4.2.6 Myoglobin expression is responsible for reduced proliferation in 231Mb cells 47

4.2.7 Mitochondrial fusion is responsible for reduced proliferation in 231Mb cells 48

4.2.8 Myoglobin expression causes cell cycle arrest at the G1/S phase transition of the cell cycle 49

4.2.9 Myoglobin-expressing tumors have lower end-tumor volume and weight than control tumors 52

4.2.10 Myoglobin-expressing tumors have a fused mitochondrial phenotype .. 53

4.2.11 Myoglobin-expressing tumors show cell cycle arrest at the G1/S phase transition 55

4.2.12 231Mb cells and myoglobin-expressing tumors have decreased parkin expression 56

4.2.13 Myoglobin expression reduces mitofusin ubiquitination 58

4.2.14 231Mb cells have cytosolic but not mitochondrial ROS 60

4.2.15 Myoglobin expression causes parkin oxidation in 231Mb cells 62

5.0 DISCUSSION 64

6.0 FUTURE DIRECTIONS 69

7.0 CONCLUSIONS 73

BIBLIOGRAPHY 74

LIST OF FIGURES

Figure 1. Mitochondria produce ATP and generate ROS. 2

Figure 2. Mitochondrial fission is mediated by drp1 [9]. 4

Figure 3. Mitochondrial fusion is mediated by mfn1 and mfn2 [9]..... 5

Figure 4. Myoglobin is an oxygen-binding heme protein [17]. 6

Figure 5. Procedure for *in vivo* ischemia/reperfusion simulation in the heart in a murine model. Ischemia was simulated by ligating the left coronary artery for 30 minutes followed by 24 hours of reperfusion. Nitrite was given 24 hours prior to reperfusion (PC) or immediately before (acute) [42]. 25

Figure 6. Nitrite significantly reduces infarct size after ischemia/reperfusion. After 30 minutes of ischemia and 24 hours reperfusion, nitrite was able to protect the heart against tissue damage regardless of whether it was given 24 hours before the reperfusion period or immediately before [42]. 26

Figure 7. Procedure for *in vivo* ischemia/reperfusion simulation in the heart in a murine model. Ischemia was simulated by ligating the left coronary artery for 30 minutes followed by 24 hours of reperfusion. Nitrite was given 5 minutes before reperfusion [43]. 27

Figure 8. Nitrite significantly reduces infarct size in wild type (Mb+/+) but not myoglobin deficient (Mb-/-) mice after ischemia/reperfusion. Under control conditions, there is no significant difference between Mb+/+ and Mb-/- mice in infarct size. When nitrite is given, infarct size is significantly reduced in Mb+/+ mice but not Mb-/- mice [43]. 27

Figure 9. Nitrite treatment significantly reduces ROS production in isolated mitochondria after ischemia/reperfusion. Amplex Red measurement of ROS generation over time showed that after ischemia reperfusion, significant ROS are generated (blue dots). When treated with 20 μM nitrite (red dots), ROS production is reduced almost to that of control levels (green dots) [42]. 28

Figure 10. Nitrite treatment significantly increases complex I S-nitrosation. Treating isolated mitochondria with 480 nmol nitrite significantly increases mitochondrial protein S-nitrosation (top). Further analysis revealed this S-nitrosation occurs at complex I of the electron transport chain (bottom) [42]. 29

Figure 11. Nitrite S-nitrosates the ND3 subunit of complex I to inhibit ROS production during reperfusion. Nitrite S-nitrosates the ND3 subunit of complex I, resulting in its inactivation, which inhibits ROS production during reperfusion. Complex I can then be reduced and return to is active form [47]..... 30

Figure 12. CHO cells were successfully transfected to stably express human myoglobin (CHOMb). 31

Figure 13. Stable transfection of myoglobin in CHO cells does not alter overall cell morphology. Bright field images show CHOR cells (left) transfected with an empty vector and CHOMb cells (right) transfected to stably express human myoglobin. 32

Figure 14. Procedure for simulating ischemia/reperfusion *in vitro*. CHOR and CHOMb cells were subjected to 1 hour of hypoxia (1% O_2) followed by 2 hours of reoxygenation (20% O_2) with 5 μM nitrite supplemented before reoxygenation. Cell death was then quantified by measuring LDH released into the cell media. 33

Figure 15. Rationale behind lactate dehydrogenase (LDH) release assay. The rate of NADH oxidized to NAD^+ is measured, which is directly correlated to the amount of LDH in the media 33

Figure 16. Nitrite significantly reduces cell death after ischemia/reperfusion injury in CHOMb cells. After ischemia/reperfusion, CHOR and CHOMb cells experience the same level of cell death under control conditions. When 5 μM nitrite is supplemented, cell death is significantly reduced in CHOMb but not CHOR cells. Data are represented as LDH in the media as a percent of total LDH. Data are represented as mean ± SEM. (# $p<0.05$). 34

Figure 17. Protein S-nitrosation in the whole cell and mitochondria in CHOR and CHOMb cells after nitrite treatment. Nitrite treatment increases S-nitrosation levels in the whole cell and mitochondria of CHOMb but not CHOR cells. (* $p<0.01$) 35

Figure 18. Procedure for transfecting CHOR an CHOMb cells and simulation of ischemia/reperfusion *in vitro.* CHOR and CHOMb cells were transfected with control or NDUFAF1 siRNA and subjected to 1 hour of hypoxia (1% O_2) followed by 2 hours of reoxygenation (20% O_2) with 5 μM nitrite supplemented before reoxygenation. Cell death was then quantified by measuring LDH released into the media..... 36

Figure 19. Silencing complex I eliminates nitrite's protective effects in CHOMb cells. When transfected with control siRNA, nitrite significantly reduces cell death in CHOMb but not CHOR cells. When transfected with NDUFAF1 siRNA, the protection previously mediated by nitrite in CHOMb cells is eliminated. Two-way ANOVA with Bonferroni correct was used to determine significance. Data are presented as mean ± SEM. (# $p<0.05$; * $p<0.01$)..... 37

Figure 20. Myoglobin mediates cell survival through reduction of nitrite to nitric oxide to S-nitrosate complex I and inhibit ROS production. 38

Figure 21. Patients with myoglobin positive tumors (Mb+) have significantly better survival than patients with myoglobin negative (Mb-) tumors [22]..... 39

Figure 22. 231 cells were successfully transfected to stably express human myoglobin (231Mb) 40

Figure 23. Stable transfection of myoglobin in 231 cells does not alter overall cell morphology. Bright field images show 231 control cells (left) and 231Mb cells (right) transfected to stably express human myoglobin. 40

Figure 24. 231Mb cells proliferate significantly less than 231 control cells measured by 24-hour ^3H thymidine incorporation. 231 proliferation rates are normalized to 1.00 and 231Mb rates represented as a percentage of 231. Data are presented as mean ± SEM. (* $p<0.01$). 41

Figure 25. Myoglobin expression significantly reduces cell migration. Cell migration was measured by a 24-hour scratch assay with the percent scratch closure calculated at the 24-hour time point. Representative images are shown in A and quantification shown in B. Data are presented as mean ± SEM. (# $p<0.05$)..... 42

Figure 26. Myoglobin expression does not increase apoptosis. Flow cytometry analysis of annexin V staining shows no significant difference between 231 and 231Mb cells. Data are presented as mean ± SEM. ($p=0.2$)..... 43

Figure 27. 231Mb cells have significant mitochondrial fusion. TOM20 staining of the outer mitochondrial membrane of 231 (A) and 231Mb (B) cells shows 231 cells have small, fragmented mitochondria whereas 231Mb cells have fused mitochondria. 44

Figure 28. 231Mb cells show significantly greater mitochondria interconnectivity by electron microscopy. Representative electron microscopy images of mitochondria of 231 and 231Mb (A) cells imaged at 15,000X and ImageJ quantification (B) show 231 control cells have small, fragmented mitochondria while 231Mb cells have fused, elongated mitochondria. Mitochondria interconnectivity is presented as mean ± SEM. (# $p<0.05$). 45

Figure 29. Mfn 1 & 2 are upregulated and drp1 downregulated in 231Mb cells. Western blot and densitometry quantification shows 231Mb cells have significantly greater mfn1 expression (* $p<0.01$), a strong trend for increased mfn2 expression, and significantly lower expression of drp1 (# $p<0.05$) than 231 control cells. Protein expression is normalized to β-actin expression and represented as mean ± SEM. 46

Figure 30. Myoglobin expression is associated with mitochondrial fusion and reduced cell proliferation..... 47

Figure 31. Silencing myoglobin by siRNA transfection in 231Mb cells restores proliferation. When 231 and 231Mb cells are transfected with control siRNA, 231Mb cells proliferate significantly less than 231 control cells (** $p<0.001$). When myoglobin is silenced, proliferation is restored in 231Mb cells (*** $p<0.0001$). Proliferation rates are normalized to 231 and represented as a percent of 231 control group. Data are presented as mean ± SEM. 48

Figure 32. Silencing mfn 1 & 2 by siRNA transfection restores proliferation of 231Mb cells. When 231 and 231Mb cells are transfected with control siRNA, 231Mb cells proliferate significantly less than 231 control cells (** $p<0.001$). When mfn 1 & 2 are silenced, proliferation is restored in 231Mb cells (*** $p<0.0001$). Proliferation rates are normalized to 231 and represented as a percent of 231 control group. Two-way ANOVA with a Bonferroni correction was used to determine significance. Data are presented as mean ± SEM. 49

Figure 33. Cells progressing from G2 to M phase of the cell cycle have fragmented mitochondria and cells progressing G1 to S phase have elongated, fused mitochondria [48, 49]..... 50

Figure 34. 231Mb cells have significantly lower cyclin E expression and significantly greater p21 expression. Densitometry analysis of cyclin E and p21 expression levels show 231Mb cells have significantly lower cyclin E expression (A) and significantly higher p21 expression (B). Protein expression is normalized to β-actin or α-Tubulin expression and represented as mean ± SEM. (# $p<0.05$; * $p<0.01$) 51

Figure 35. Myoglobin expression is associated with mitochondrial fusion, which causes cell cycle arrest and reduces cell proliferation. 52

Figure 36. Myoglobin-expressing tumors show a strong trend for reduced end tumor volume and weight. N=5 mice per group. Data are presented as mean ± SEM. 53

Figure 37. Myoglobin-expressing tumors have fused mitochondria. Electron microscopy analysis of tumor tissue show that myoglobin-expressing tumors have elongated, fused mitochondria whereas control tumors have punctate, fragmented mitochondria (A). Mitochondria interconnectivity was quantified by the ratio of area to perimeter, with myoglobin tumors having significantly greater mitochondrial interconnectivity. Data are expressed as mean ± SEM. (#$p<0.05$)..... 54

Figure 38. Myoglobin-expressing tumors have significantly lower cyclin E expression and significantly greater p21 expression. Western blot analysis of cyclin E is shown in A and p21 in B. Protein expression is normalized to α-Tubulin expression and represented as mean ± SEM. (# $p<0.05$) 55

Figure 39. Parkin causes mitofusin ubiquitination, thereby inhibiting mitochondrial fusion. 56

Figure 40. 231Mb cells and myoglobin-expressing tumors have significantly lower parkin expression and control cells and tissue. Protein expression is normalized to β-actin expression and represented as mean ± SEM. (# $p<0.05$; * $p<0.01$)..... 57

Figure 41. Myoglobin could cause a reduction in parkin expression to inhibit mitofusin ubiquitination and drive mitochondrial fusion..... 58

Figure 42. 231Mb cells have less mfn1 ubiquitination than 231 control cells. Western blot and densitometry analysis show mfn1 is ubiquitinated less in 231Mb cells than in 231 cells. Ubiquitin levels are normalized to mfn1 expression in each cell type. Data are presented as mean ± SEM. (# $p<0.05$). 59

Figure 43. Myoglobin expression causes a reduction parkin expression to decrease mfn1 ubiquitination and drive mitochondrial fusion to cause cell cycle arrest and reduce cell proliferation..... 60

Figure 44. Myoglobin expression does not change amount of mitochondrial-produced ROS. As measured by the MitoSOX™ Red assay, there is no significant difference in mitochondrially-produced ROS in 231 and 231Mb cells. ($p=0.5$) 61

Figure 45. 231Mb cells do not produce mitochondrial ROS. As measured by the Amplex® Red assay and treating with mitoTEMPOLto scavenge mitochondrially-produced ROS, ROS production is not reduced in 231Mb cells. (** $p<0.001$, * $p<0.01$)..... 62

Figure 46. Parkin oxidation is significantly increased in 231Mb cells. Biotin levels are normalized to parkin levels in the cell. Data are presented as mean ± SEM. (# $p<0.05$) 63

NOMENCLATURE

ATP – Adenosine triphosphate

BSA – Bovine serum albumin

Cu/Zn SOD – Copper/Zinc Superoxide Dismutase

H_2O_2 – Hydrogen peroxide

HBSS – Hank's Buffered Saline Solution

HRP – Horseradish Peroxidase

MnSOD – Manganese Superoxide Dismutase

NEM – N-ethylmaleimide

PBS – Phosphate Buffered Saline

PFA – Paraformaldehyde

ROS – Reactive Oxygen Species

STE – Sodium Chloride-TRIS-EDTA

TCA – Trichloroacetic Acid

TCEP – tris(2-carboxyethyl)phosphine

PREFACE

First and foremost, I would like to thank my thesis advisor Dr. Sruti Shiva for her guidance, support, and the opportunities she has given me during my time in her lab. I could not have asked for a better mentor as my time as a graduate student. I would also like to thank my thesis committee, Dr. Sanjeev Shroff, Dr. Michael Lotze, and Dr. Adam Straub for the feedback they have provided me with during this project. I would also like to thank everyone in the Shiva lab, without them this project would not have been possible. A special thanks to Kelly Quesnelle, who started this project and trained me during my first few months in the lab. Finally, I would like to thank my friends and family for their continuous support and encouragement, without them I would not be where I am today.

1.0 INTRODUCTION

The small oxygen-binding heme protein myoglobin has long been recognized to regulate mitochondria in skeletal and cardiac muscle cells through oxygen delivery. Myoglobin is now recognized for its expression in tissues beyond skeletal muscle cells including smooth muscle and some cancer tumors. Additionally, myoglobin can react with reactive nitrogen species to modulate mitochondrial function independent of oxygen delivery. This thesis will investigate how these novel functions of myoglobin and how they contribute to regulation of mitochondria in two pathological models.

1.1 MITOCHONDRIA

Mitochondria were first discovered by Altmann in 1886, with their structure first recognized in 1857, and were initially thought to be parasites within the cell. Nearly 100 years after their initial discovery, Peter Mitchell first described the chemiosmotic theory in 1961 [1]. Together with the findings of Warburg and Keilin, this discovery describes how electrons from NADH and $FADH_2$ enter complexes I and II of the respiratory chain embedded within the inner mitochondrial membrane. These electrons are then transferred to complex III through ubiquinone and finally by cytochrome c to complex IV (cytochrome *c* oxidase) where oxygen is reduced to water. Simultaneously, protons are pumped from the matrix of the mitochondria into the inter-

membrane space, creating an electrochemical gradient (Δμ) and a buildup of protons in the intermembrane space. This gradient drives the re-entry of protons into the mitochondrial matrix via complex V (ATP synthase). As protons move back into the matrix, ADP and inorganic phosphate combine, generating ATP. Mitochondria are known for their role in energy production, as they are typically referred to as "powerhouses of the cell", generating the necessary amount of ATP to sustain the metabolic functions of the cell (Figure 1) [2, 3].

In addition to energy production, mitochondria are now recognized to play an important role in maintaining cellular homeostasis through generation of reactive oxygen species (ROS) and initiation of the apoptotic cascade. While the majority of electrons pass through complexes I through IV of the electron transport chain, approximately 2% of electrons leak out prematurely, which typically occurs at complexes I and III. These electrons can then oxidize oxygen, forming superoxide (O_2^-), which is rapidly converted to hydrogen peroxide (H_2O_2) by manganese superoxide dismutase (MnSOD) in the mitochondrial matrix and copper/zinc superoxide dismutase (Cu/Zn SOD) in the cytosol [4].

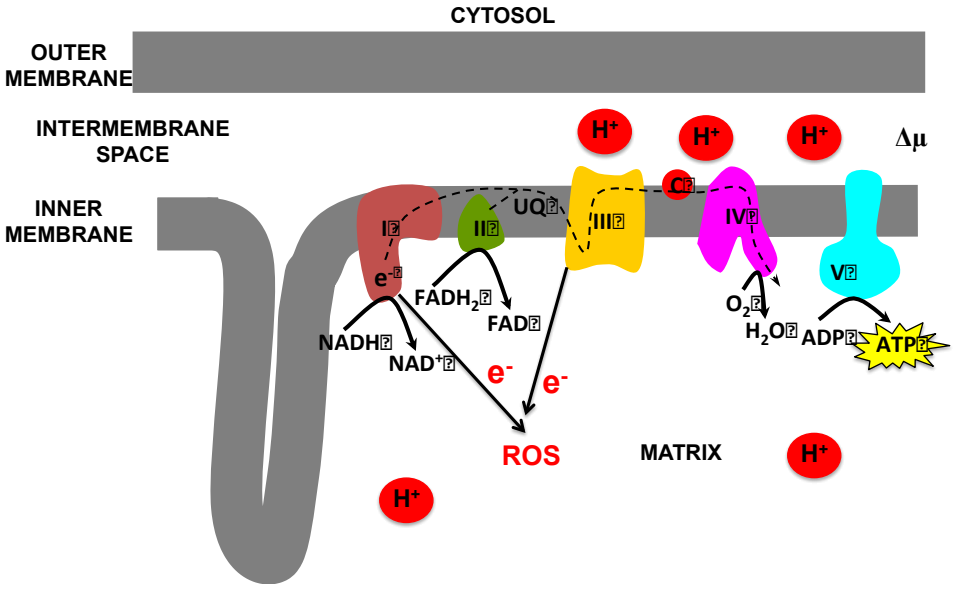

Figure 1. Mitochondria produce ATP and generate ROS.

ROS were once thought to only be associated with tissue damage and pathological conditions. However, low levels of ROS are now recognized to be important in a variety of cellular signaling processes including cell growth and proliferation as well as the inflammatory response. Additionally, ROS play a significant role in protection in the heart from ischemia/reperfusion injury, which will be addressed in Aim 1 [5]. It should be noted, however, that high levels of ROS cause protein and lipid oxidation and DNA damage, resulting in cell death and tissue damage [6].

Another important function of mitochondria is the initiation of the apoptotic cascade. Cytochome *c* is released from cardiolipin in the inner mitochondrial membrane into the cytosol, where it binds apoptotic protease activating factor-1 (APAF-1), forming an apoptosome. The apoptosome then binds and cleave procaspase 9, resulting in its fully activated form, which subsequently stimulates the caspase cascade and commits the cell to apoptosis [7].

1.1.1 Mitochondria are dynamic structures

In order to maintain the energy demands of the cell, mitochondria constantly come together (fusion) and break apart (fission). These fission and fusion events are mediated by guanosine triphosphotases (GTPases) of the dynamin protein family. Specifically, fission is mediated by dynamin related protein-1 (drp1) while fusion is mediated by the mitofusins (mfn) 1 and 2 [8].

Mitochondrial fission typically occurs in stressed cells and it has been shown to occur almost simultaneously with release of cytochrome *c* from the inner mitochondrial membrane. Moreover, fission occurs to segregate damaged mitochondria from fully functioning mitochondria, allowing damaged mitochondria to be targeted for autophagy. Additionally,

fission is crucial in actively growing and diving cells to provide each daughter cell with appropriate number of mitochondria [8].

As shown in Figure 2, fission occurs when drp1 is recruited from the cytosol to the mitochondria, forming spiral-like structures around the membrane. These proteins constrict the mitochondria, severing both inner and outer membranes and forming two separate mitochondria [8].

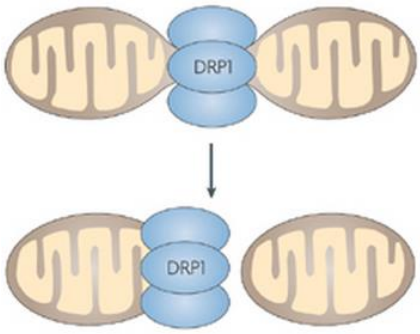

Figure 2. Mitochondrial fission is mediated by drp1 [9].

Mitochondrial fusion most commonly occurs to maximize respiratory capacity. It has been shown that mitochondria become increasingly fused when cells are forced to undergo oxidative phosphorylation by withdrawing glucose as a source for glycolysis [10]. The mitofusin proteins, mfn 1 and 2 are responsible for mediating fusion and are localized to the outer mitochondrial membrane. As shown in Figure 3, these proteins direct mitochondrial fusion by forming homo- and hetero-oligomeric complexes, tethering two membranes together, forming a single mitochondrion [8, 10].

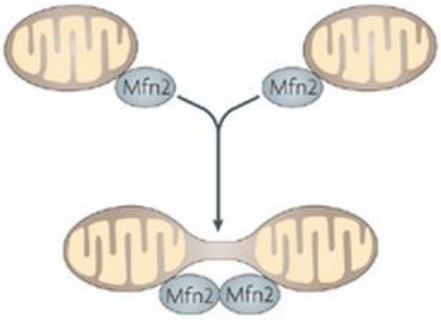

Figure 3. Mitochondrial fusion is mediated by mfn1 and mfn2 [9].

1.2 MYOGLOBIN

The small protein myoglobin is one of the most well characterized proteins to date. Myoglobin was first discovered as a muscle pigment, referred to as muscle hemoglobin, by Mörner in 1879 [11]. Mörner distinguished myoglobin from hemoglobin by their different absorbance spectra and suggested the name *monochrome* for this protein. In 1921, the term *myoglobin* was coined by Günther who confirmed Mörner's results [12, 13]. In 1958, John Kendrew was the first to resolve the three-dimensional structure of myoglobin by X-ray crystallography, making myoglobin the first protein to be described at the atomic level. In 1962, John Kendrew shared the Nobel Prize in chemistry with Max Perutz for this discovery [14].

1.2.1 Myoglobin structure and localization

Myoglobin is a 17 kD monomeric heme protein consisting of a single polypeptide chain of 153 amino acids [15]. It is a member of the globin superfamily, meaning it contains a globin fold comprising a series of eight alpha helices [3, 16]. These alpha helices are folded around a hydrophobic core that contains the heme prosthetic group, which consists of a porphyrin ring bonded to a central iron atom by four nitrogen atoms and the proximal histidine residue at the fifth coordination site (His 93), as shown in Figure 4 [3, 17]. The outside surface of the myoglobin protein is composed primarily of hydrophilic residues, allowing the molecules to easily move past one another in a concentrated solution [18]. Oxygen, as well as small ligands such as carbon monoxide (CO) and nitric oxide (NO), bind myoglobin at the sixth coordinate site of the heme iron. The distal histidine (His 64) becomes important in the binding of these small molecules, as it facilitates binding through hydrogen bonding [19].

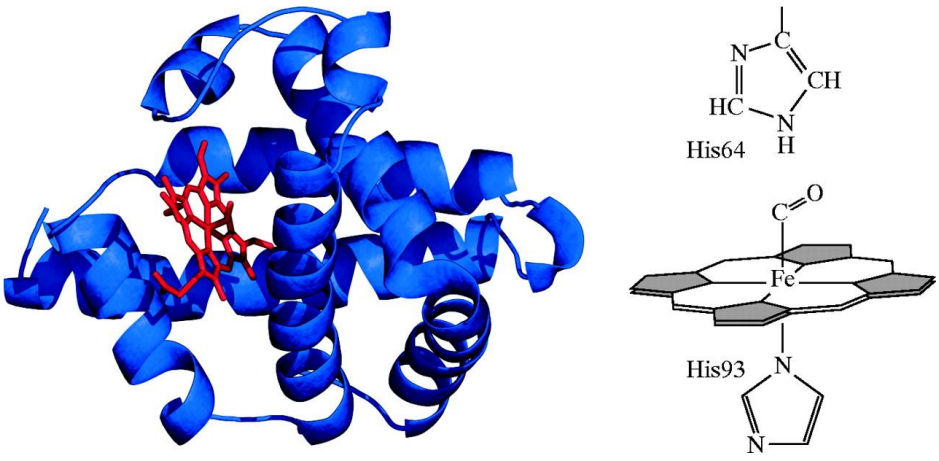

Figure 4. Myoglobin is an oxygen-binding heme protein [17].

Myoglobin is known for its expression in cardiac and skeletal muscle of all large vertebrates, with a relatively preserved amino acid sequence and three-dimensional structure. The myoglobin content in cardiac and skeletal muscle is closely correlated with cytochrome *c* oxidase expression, capillary density, and increases dramatically with exercise. The basal myoglobin concentration in cardiac muscle is approximately 200-300 μmol kg^{-1} wet weight while the concentration in skeletal muscle is much higher at 400-500 μmol kg^{-1} wet weight [16, 18]. Interestingly, myoglobin has recently been discovered in low concentrations in smooth muscle cells [20, 21] as well as tumor tissue of non-muscle origin [22-24]. Early investigation of myoglobin expression in cancer revealed myoglobin improves patient outcomes [22]. However, the role of myoglobin expression in these tissues has not been elucidated. The effect of myoglobin expression on mitochondria in cancer cells will be investigated in Aim 2.

1.3 REGULATION OF MITOCHONDRIA BY MYOGLOBIN

1.3.1 Myoglobin is an oxygen storage protein

Myoglobin's role in oxygen storage was discovered fairly early and remains its most well-known and accepted function. Myoglobin has a very high affinity for oxygen, with a P_{50} of 3.1μM [3, 25]. In tissues requiring significant energy production such as cardiac muscle, myoglobin is present in very high concentrations, allowing for sustained muscle contraction. Studies have shown that at the onset of contraction, a new deoxygenated steady-state is reached within 20-40 seconds, suggesting that myoglobin releases oxygen to respiring mitochondria, driving muscle contraction [16, 26].

1.3.2 Myoglobin-facilitated oxygen diffusion

Another, somewhat controversial function of myoglobin is its ability to bind and transport oxygen within the cell to hypoxic respiring mitochondria. This function of myoglobin was first reported by Wittenberg in which he described how oxygen diffusion is enhanced from the sarcolemma to the mitochondrion due to myoglobin's ability to quickly bind oxygen, diffuse through the cell, and unload oxygen to respiring mitochondria [27-29].

In 1996, Johnson et al. showed that oxygen diffuses faster in myoglobin-containing solutions than in non-myoglobin solutions [29, 30]. Due to its high affinity for oxygen, myoglobin is able to quickly bind oxygen as it diffuses from the capillary into the cell, transport it to mitochondria, and finally release oxygen as oxygenated myoglobin comes to equilibrium with deoxygenated myoglobin. In 2000, Takahashi et al. demonstrated in isolated cardiomyocytes that significant intracellular gradients are developed when stimulating mitochondrial respiration. These gradients extend from the core of the cell, which is anoxic, to the plasma membrane. Moreover, upon inactivation of cytosolic myoglobin with 5 nM $NaNO_2$ treatment, the anoxic core region expands significantly. These results suggest myoglobin binds oxygen at the plasma membrane and carries it deeper within the cell where it unloads oxygen to respiring mitochondria. Thus, by carrying oxygen away from the plasma membrane, myoglobin effectively extends the oxygen gradient within the cell [31].

In 2001, with the generation of myoglobin-deficient mice (Mb-/-), Merx et al. showed that oxygen consumption in cardiomyocytes from Mb-/- mice is lower than oxygen consumption from wild type (WT) cardiomyocytes when ambient PO_2 is decreased from 40mmHg to 8mmHg.

Therefore, in WT cardiomyocytes myoglobin releases bound oxygen to respiring mitochondria, allowing for continued oxygen consumption as ambient PO_2 decreases. In Mb-/- cardiomyocytes, however, myoglobin is not present to release its stored oxygen to mitochondria, resulting in decreased oxygen consumption [32].

1.3.3 Myoglobin reacts with reactive nitrogen species to modulate mitochondrial function

Nitrite is present in concentrations of 100-250 nM in the plasma and 1-10 μM in tissue and is now recognized as a bioavailable storage pool for the signaling molecule nitric oxide (NO). Nitrite can be reduced to nitric oxide through several mechanisms including acidic disproportionation, enzymatic conversion by xanthine-oxidoreductase, and mitochondrial enzymes. It is well known that deoxyhemoglobin has nitrite reductase activity, able to react with bioavailable nitrite in the blood, generating nitric oxide, which subsequently causes vasodilation [33, 34]. In 2007 it was shown that in low oxygen concentrations, deoxymyoglobin also has nitrite reductase activity, which occurs by the reaction below, converting ferrous (Fe^{2+}) myoglobin to metmyoglobin (Fe^{3+}) and generating nitric oxide. Notably, the reduction of nitrite by deoxymyoglobin occurs approximately 36 times faster than deoxyhemoglobin due to its low heme redox potential [35].

$$deoxyMb(Fe^{2+}) + NO_2^- + H^+ \rightarrow metMb(Fe^{3+}) + NO$$

Nitric oxide also reacts with myoglobin, however this occurs under normal oxygen tensions when myoglobin is oxygenated. The ability of nitric oxide to react with heme centers is now recognized as one of its most important characteristics. As shown in the reaction below, nitric oxide reacts with oxygenated myoglobin converting ferrous (Fe^{2+}) myoglobin to metmyoglobin (Fe^{3+}) and generating nitrate [36, 37].

$$Mb(Fe^{2+})O_2 + NO \rightarrow metMb(Fe^{3+}) + NO_3^-$$

1.3.4 Nitric oxide regulates mitochondria

It the late 1990's, nitric oxide was found to modulate mitochondrial function through inhibition of cytochrome *c* oxidase (complex IV) in low oxygen conditions. It has now been shown that bioavailable nitrite reacts with deoxymyoglobin, producing nitric oxide, which reversibly binds cytochrome *c* oxidase at the binuclear center (Cu_B/cytochrome a_3) active site, inhibiting respiration. Because nitric oxide must compete with oxygen for binding to cytochrome *c* oxidase, this inhibition is especially pronounced at low oxygen tensions [38].

In 2001, Brunori proposed that the reaction of myoglobin and nitric oxide in normoxia is important to avoid inhibition of cytochrome *c* oxidase by nitric oxide. This becomes extremely important in cardiac muscle, which is under continuous energy demand due to constant contraction. Therefore, mitochondria have to continually respire to generate the necessary amount of ATP to sustain this contraction. Thus, in normoxia, myoglobin scavenges nitric oxide, allowing respiration to continue uninhibited [36]. Myoglobin's ability to generate nitric oxide is also very important. When oxygen is limited, inhibition of respiration by nitric oxide serves as a

mechanism to conserve the little oxygen present in the tissue and extend oxygen gradients deeper within the tissue [39]. Therefore, under normoxic conditions, myoglobin will scavenge nitric oxide, thereby allowing respiration to continue and in hypoxia myoglobin will generate nitric oxide in an attempt to preserve oxygen and extend oxygen gradients within the cell [41]. These novel reactions of myoglobin become particularly important in the context of ischemia/reperfusion injury, which will be the focus of Aim 1.

2.0 RESEARCH OBJECTIVES

While myoglobin and mitochondria have been studied extensively in the context of oxygen delivery and utilization, it has only recently been recognized that they interact by mechanisms not involving oxygen delivery. As described in the previous section, myoglobin has many functions besides oxygen storage and delivery and is expressed in more tissues than just skeletal muscle. Thus, the focus of this thesis is to elucidate the mechanisms by which myoglobin regulates mitochondrial function beyond oxygen storage and delivery.

Aims and Hypotheses

Specific Aim 1: Determine whether myoglobin mediates nitrite dependent protection in ischemia/reperfusion.

Hypothesis: Myoglobin catalyzes the reduction of nitrite to nitric oxide to mediate complex I S-nitrosation in ischemia/reperfusion.

Specific Aim 2: Investigate the effect of myoglobin expression on mitochondrial dynamics and cell proliferation in breast cancer

Hypothesis: Myoglobin-dependent changes in mitochondrial dynamics and function modulates cell survival and proliferation in normoxic breast cancer cells.

3.0 EXPERIMENTAL METHODS

3.1 REAGENTS

All reagents were purchased from Sigma-Aldrich (St. Louis, MO, USA) unless noted. MDA-MB-231 cells were purchased from ATCC (Rockville, MD, USA).

3.2 STABLE TRANSFECTION OF MYOGLOBIN IN MDA-MB-231 CELLS

GFP-tagged human myoglobin (GFP-Mb) was purchased from Origene (RG212352, Rockville, MD, USA). Bacterial transformation was performed using several different DNA concentrations. DNA was added to 100µl MDA-MB-231 cells (231) and incubated at 42°C for 45 seconds followed by incubation on ice for 2 minutes. 900µl S.O.C medium was added to tubes and allowed to shake at 225 RMP at 37°C for 1 hour. 200µl of this mixture was spread on agar plates containing 100µg/µl ampicillin and incubated overnight at 37°C. Viable colonies were chosen and glycerol stocks prepared. DNA was then purified using a Qiagen plasmid kit (Venlo, Netherlands).

231 cells were transfected with GFP-Mb DNA using Lipofectamine 2000 (Life Technologies, Grand Island, NY, USA). Approximately 48 hours after transfection, cells were passaged in media containing geneticin (Life Technologies) to select only for cells resistant to the antibiotic. Single cells from resistant colonies were transferred to 96-well plates to confirm they were able to yield antibiotic-resistant colonies, which were then expanded.

3.3 MYOGLOBIN-EXPRESSING CHO CELLS

CHO cells stably transfected to express human myoglobin were generated by Dr. Dara Frank and given as a gift from Dr. Neil Hogg from the Medical College of Wisconsin.

3.4 CELL CULTURE

231 and myoglobin-expressing 231 cells (231Mb) were cultured in Dulbecco's Modified Eagle Medium (Invitrogen, Grand Island, NY, USA) supplemented with 10% fetal bovine serum (FBS) (Life Technologies), 1% penicillin-streptomycin (Lonza, Basel, Switzerland), and 1% Geneticin (DMEM growth medium). Chinese hamster ovary (CHO) cells and myoglobin-expressing CHO cells (CHOMb) were cultured in Ham's F12 Nutrient Mixture (Invitrogen) supplemented with 10% FBS, 1% penicillin-streptomycin, 1% Geneticin, and 0.001% Hemin. Cells were stored in an incubator maintained at 37°C, 21% O_2, and 5% CO_2.

3.5 BRIGHT FIELD IMAGING

Bright field images were taken with a Zeiss Axiovert 40 CFL microscope (Carl Zeiss Microscopy, Thornwood, NY, USA) and analyzed with AxioVision software Rel. 4.8 (Carl Zeiss Microscopy).

3.6 S-NITROSATION DETECTION

S-nitrosation was detected by tri-iodide based reductive chemiluminescence in the presence and absence of acidified sulfanilamide as previously described [42]. Briefly, after treatment of cells with nitrite (in the presence and absence of myoglobin), SNO was stabilized with 100 mM Diethylenetriaminopentaacetic acid (DTPA), 4 mM Cyanide/ferricyanide (III), 10 mM N-Ethylmaleimide, and 1% NP-40. The sample was then divided into three parts: one left untreated, one treated with 10% acidified sulfanilamide (v/v) to eliminate nitrite, and one treated with 5mM mercuric chloride and 10% acidified sulfanilamide to eliminate SNO and nitrite. The fractions were then injected into a triiodide-containing vessel that was connected to an NO chemiluminescence detector (Sievers).

3.7 CHO NDUFAF1 TRANSFECTION

CHOR and CHOMb cells were allowed to grow to approximately 70% confluence. Cells were washed once with 1X PBS and media replaced with Opti-MEM® reduced serum medium (Invitrogen) Cells were transfected with either control (sc-37007, Santa Cruz Biotechnology, Santa Cruz, CA) or NDUFAF1 (SI01602251, Qiagen, Hilden, German) targeted siRNA using Lipofectamine 2000 transfection reagent (Invitrogen).

3.8 ISCHEMIA/REPERFUSION SIMULATION

Ischemia was simulated by incubating cells in hypoxia (1% O_2, 5% CO_2) for two hours in modified Esumi Buffer (137 mmol/L NaCl, 12 mmol/L KCl, 0.5 mmol/L MgCl2, 0.9 mmol/L CaCl2, 20 mmol/L HEPES; 20 mmol/L 2-deoxy-D-glucose (2-DG), pH 6.2). Reperfusion was simulated by reoxygenating cells in 20% O_2 (5% CO_2) in the same modified Esumi Buffer for one hour. Nitrite-treated cells were reoxygenated in 20% O_2 (5% CO_2) in modified Esumi Buffer supplemented with 5μM NO_2^- for one hour.

3.9 LACTATE DEHYDROGENASE ACTIVITY ASSAY

Lactate dehydrogenase (LDH) activity in the media was determined by kinetically measuring the rate of NADH oxidation to NAD^+ using a Synergy plate reader (BioTek Instrument Inc. Winooski, VT) at 340nm.

3.10 WESTERN BLOT

Samples were lysed in buffer containing 20 mM Tris/HCl pH 7.5, 1 mM EDTA, 150 mM NaCl, 1% NP40, 1% sodium deoxycholate, 1X Phenylmethylsulfonyl fluoride (PMSF) and 1X protease inhibitors. Tissue samples were briefly homogenized prior to lysis. Protein concentrations were determined by a BCA assay (Pierce, Rockford, IL, USA). Cell lysates were prepared and denatured at 95°C. Equal amounts of protein were loaded in gels ranging in percentages from 7-15 and proteins separated by SDS-PAGE. Proteins were then transferred to a nitrocellulose (Bio-Rad Laboratories, Hercules, CA, USA) or polyvinylidene difluoride (PVDF) membrane (Bio-Rad Laboratories). After transfer, membranes were incubated in LI-COR® Blocking Buffer (LI-COR Biosciences, Lincoln, NE, USA) diluted 1:1 in PBS at room temperature for one hour to reduce nonspecific antibody binding. Membranes were incubated with primary antibodies diluted 1:500 in a 5% BSA PBS solution for 2 hours at room temperature or overnight at 4°C. Antibodies used include NDUFAF1 (sc-86755, Santa Cruz Biotechnology), mfn1 (sc-50330, Santa Cruz Biotechnology), drp1 (sc-32898, Santa Cruz Biotechnologies), parkin (#2132, Cell Signaling Technology, Danvers, MA, USA), p21 (BD Pharmingen, San Jose, CA, USA), cyclin E (sc-481, Santa Cruz Biotechnology), or biotin (B7653, Sigma). After incubation with primary antibody, blots were washed 5 times for 5 minutes in 0.01% TBST and incubated with appropriate fluorophore conjugated secondary antibodies diluted 1:10,000 in a 5% BSA PBS solution for one hour at room temperature. Membranes were then washed for 5 times for 5 minutes in TBST and imaged with a LI-COR® odyssey imaging system (LI-COR®, Lincoln NE, USA).

Images were analyzed using LI-COR® odyssey infrared imaging software version 3.0 (LI-COR®). To normalize protein concentration to total protein, blots were stripped with LI-COR® stripping buffer (LI-COR® Biosciences), washed, and reprobed with antibodies against either α-Tubulin (CP06, Calbiochem, Billerica, MA, USA) or β-actin (A5316, Sigma).

3.11 ^{3}H THYMIDINE INCORPORATION

Cells were plated in a 24-well plate and incubated with media containing ^{3}H Thymidine (5μCi/mL) for 24 hours. To determine amount of ^{3}H thymidine incorporation, cells were washed with 1mL 1X PBS and incubated in 5% TCA at 4°C for 30 minutes. Cells were then washed once with 5% TCA and 1X PBS and incubated in 0.2N NaOH at room temperature for 30 minutes to precipitate DNA. Each sample was then added to a scintillation tube containing 4mL scintillation fluid (Perkin Elmer, Waltham, MA, USA) and read in a scintillation counter.

3.12 CRYSTAL VIOLET STAINING

Media was aspirated from 24-well cell plates, 0.25% crystal violet was added to cover the bottom of the plate (~100μl), and put on a shaker for 30 minutes. Crystal violet was then washed off by dunking the plate in cold water two times and the plate was allowed to dry overnight. Crystal violet was dissolved by adding 1% SDS (~200μl) to the plate. Absorbance was measured in a Synergy plate reader (BioTek Instrument Inc.), which is correlated to DNA content.

3.13 SCRATCH ASSAY

Cells were plated in 6-well plates and allowed to grow approximately to 70% confluence. Plates were scratched and imaged for a 0 hour time-point. Cells were incubated at 37°C (20% O_2, 5% CO_2) for 24 hours. Cells were then imaged at the 24-hour time point. Area of the scratch was quantified with NIH ImageJ software and percent closure calculated using the equation below.

$$percent\ closure = \frac{A_{t=24} - A_{t=0}}{A_{t=0}} \times\ 100$$

3.14 APOPTOSIS MEASUREMENT

Apoptosis was measured in 231 and 231Mb cells by annexin V staining and flow cytometry analysis. Cells were trypsinized, washed with 1X PBS, and resuspended in 10X binding buffer (51-66121E, BD Pharmingen) at a concentration of approximately 1×10^6 cells/mL. Cells were then incubated with propidium iodide and annexin V (560506, BD Biosciences, San Jose, CA, USA) for 15 minutes in the dark and analyzed by flow cytometry within 1 hour.

3.15 FLUORESCENCE IMAGING

Cells plated on coverslips in a 6-well plate were first rinsed with 1X PBS and fixed in 4% PFA for 30 minutes on a shaker. Cells were then rinsed in 0.1% Triton X-100 in PBS and incubated with Li-Cor® blocking buffer diluted 1:1 in PBS for 1 hour on a shaker. Cells were stained with rabbit anti-TOM20 (sc-11415, SantaCruz Biotechnologies) diluted 1:1000 in 50% LiCor® PBS

solution overnight at 4°C. Cells were rinsed three times with 1X PBS and stained with goat anti-rabbit Cy3 secondary antibody (A10520, Invitrogen) for two hours at room temperature. Cells were imaged with a confocal microscope using a 60X objective and 3X optical zoom with a step size of 0.77μm.

3.16 TRANSMISSION ELECTRON MICROSCOPY

Cells were grown to approximately 80% confluency in a 6-well plate. Fist, cells were rinsed once with 1X PBS and fixed with 2.5% glutaraldehyde in PBS for 1 hour at room temperature on a shaker. After fixation cells were rinsed with 1X PBS 3 times for 10 minutes each. Cells were then post-fixed for 1 hour at 4° C in 1% OsO_4 with 1% potassium ferricyanide and washed 3 times in 1X PBS for 10 minutes each. Cell monolayers were dehydrated in a series of alcohol (30%, 50%, 70%, and 90%) for 10 minutes each with three washes in 100% ethanol for 15 minutes each. Cell monolayers were then incubated in epon resin 3 times for 1 hour each and samples collected using beam capsules after removal of the final epon incubation. Samples were polymerized at 37°C overnight then 60°C for 48 hours. Samples were then removed from the dish and sectioned with an ultramicrotome using a diamond knife. Samples were imaged at 25,000X using a JEOL JEM 1011 transmission electron microscope (JEOL Ltd., Tokyo, Japan).

3.17 HYDROGEN PEROXIDE MEASUREMENT

Cytosolic hydrogen peroxide (H_2O_2) levels were quantified using Amplex® Red (Life Technologies) per manufacturer's instructions. Cells were collected by trypsinizing and resuspending in STE buffer. Cells were then added to a 96-well plate and with the Amplex Red master mix (PBS, HRP, Amplex Red reagent) and the mitochondrial-targeted ROS scavenger mitoTEMPOL or STE for control groups. Fluorescence (570/585 nm) was read using a Synergy plate reader (BioTek Instrument Inc.). Data was analyzed and normalized to protein concentration determined by Pierce BCA assay (Thermo Fisher Scientific, Rockford, IL, USA).

3.18 SUPEROXIDE MEASUREMENT

Mitochondrial superoxide was measured using MitoSOX™ Red reagent (Life Technologies) per manufacturer's instructions. Cells were collected by trypsinizing and resuspending in HBSS buffer. Cells were then added to a 96-well plate and MitoSOX™ Red master mix (MitoSOX ™ Red and HBSS). Fluorescence (510/580 nm) was read immediately using a Synergy plate reader (BioTek Instrument Inc.). Data was analyzed and normalized to protein concentration determined by Pierce BCA assay.

3.19 MDA-MB-231 SIRNA TRANSFECTION

231 and 231Mb cells were plated and allowed to grow to approximately 70% confluence. Cells were washed one time with PBS and media was changed to Opti-MEM® reduced serum medium (Life Technologies). Cells were transfected with human myoglobin (sc-35995, Santa Cruz Biotechnology), mfn1 (sc-43927, Santa Cruz Biotechnology), or mfn2 (sc-43928, Santa Cruz Biotechnology) targeted siRNA using Santa Cruz siRNA Transfection Reagent (sc-29528, Santa Cruz Biotechnology) according to the manufacturer's instructions.

3.20 MFN1 IMMUNOPRECIPITATION

Cell lysates were collected and protein concentration determined by BCA assay. Lysates of equal protein concentration were incubated with 1-2μg mfn1 antibody (sc-50330, Santa Cruz Biotechnologies) at 4°C on a tumbler overnight. The next day, samples were incubated with protein A/G beads (sc-2003, Santa Cruz Biotechnology) for 1-3 hours at 4°C on a tumbler. Samples were then boiled at 95°C, beads removed by centrifugation, and separated by SDS-PAGE. Ubiquitination was detected using an ubiquitin antibody (sc-9133, Santa Cruz Biotechnology).

3.21 MEASUREMENT OF PARKIN OXIDATION BY BIOTIN SWITCH

231 and 231Mb cells were collected and reacted on ice in lysis buffer (1% SDS, 0.5% Triton-X100, 0.1mM Neocuprion in PBS) for 30 minutes. Cell lysates of equal protein concentration were treated with 20mM N-ethylmaleimide (NEM) to block free thiols. 10mM Tris (2-carboxyethyl) phosphine (TCEP) was used to reduce disulfide bonds and NEM-PEG_2-biotin to label these reduced free thiols. As positive controls, lysates and bovine serum albumin were not treated with NEM at the block step, but reacted with TCEP at the label step, which allows all cysteine residues to be tagged with biotin. Negative controls have few free thiols available to be biotin-labeled, as they are not treated with TCEP at either the blocking or label step.

Streptavidin beads were used to pull down biotinylated proteins in the albumin positive control and parkin was pulled down in the 231 and 231Mb samples using a standard immunoprecipitation procedure described previously. Samples were boiled at 95°C for 5 minutes, beads removed by centrifugation, and separated by SDS-PAGE. A biotin antibody was used to detect only biotinylated proteins.

3.22 ANIMALS

Ten 4-5 week old female NOD.CB17-Prkdc^{scid}/J mice were purchased from Jackson Laboratories (Bar Harbor, ME). Following a 3-day acclimation period, mice were placed on irradiated AIN-76A diet (Harlan-Teklad, Indianapolis, IN). Mice were fed this diet for the remainder of the study. After 1 week on diet, the mice were orthotopically injected in both inguinal mammary fat pads with 3 x 10^6 control 231 or 231Mb cells. Cells were cultured to

approximately 40-60% confluency in culture dishes. Dishes were washed with PBS, trypsinized, centrifuged at 1100 RPM for 5 minutes, and diluted to 10^8 cells/mL serum-free media. Tumor growth was measured using Vernier calipers and recorded each week beginning when tumors became measurable. Tumor volume was by using the following equation:

$$tumor\ volume\ (mm^3) = \frac{length\ \times\ width^2}{2}$$

The study was terminated when the average tumor volume in the control group approached 1.5 cm^3. At the time of sacrifice, the mice were euthanized by CO_2 overdose. Tumors were harvested from each animal and weights were recorded.

3.23 STATISTICS

All values are expresses at mean ± SEM. Single comparisons were tested for significance by a two-tailed Student's t-test. ANOVA was used when comparing multiple groups with a Bonferroni post-hoc analysis to correct for multiple comparisons. Differences were considered significant when $p<0.05$.

4.0 RESULTS

4.1 AIM 1

Nitrite, an anion ubiquitously expressed in biology, has been shown to be protective against ischemia/reperfusion injury. We can get nitrite from a variety of sources in the diet including leafy green vegetable and cured meat as well as from the oxidation of nitric oxide. It is present in physiology at approximately 100-250 nM in the plasma and 1-10 μM in tissue.

In 2007, Shiva et al. showed that nitrite is protective against ischemia/reperfusion injury in the heart. Cardiac ischemia/reperfusion injury was simulated in a murine model by ligating the left coronary artery for 30 minutes followed by 24 hours of reperfusion. As shown in Figure 5, nitrite (48 nmol) was supplemented either 24 hours prior to reperfusion (PC) or immediately before the reperfusion period (acute) [42].

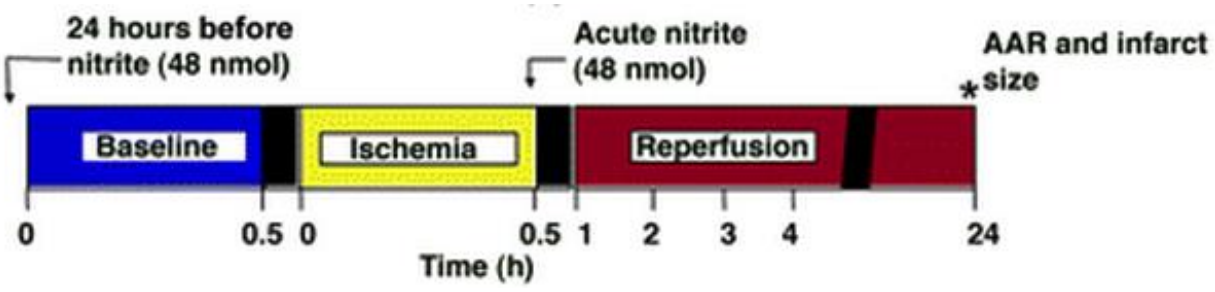

Figure 5. Procedure for *in vivo* ischemia/reperfusion simulation in the heart in a murine model. Ischemia was simulated by ligating the left coronary artery for 30 minutes followed by 24 hours of reperfusion. Nitrite was given 24 hours prior to reperfusion (PC) or immediately before (acute) [42].

These results showed that regardless of when nitrite was given, it was protective against tissue damage and significantly reduced the infarct size in the heart (Figure 6) [42].

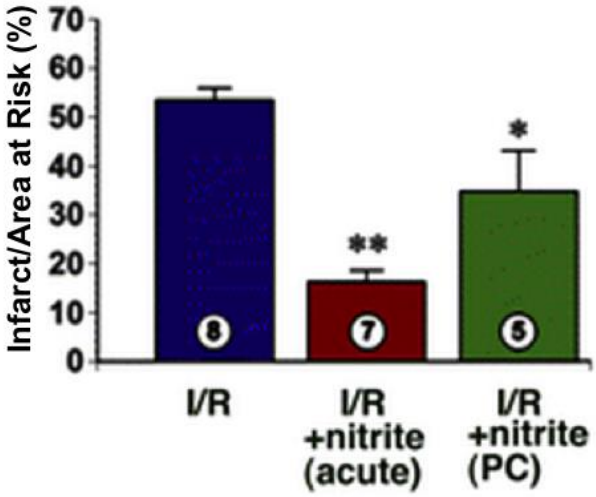

Figure 6. Nitrite significantly reduces infarct size after ischemia/reperfusion. After 30 minutes of ischemia and 24 hours reperfusion, nitrite was able to protect the heart against tissue damage regardless of whether it was given 24 hours before the reperfusion period or immediately before [42].

It was further shown by Hendgen-Cotta et al that myoglobin is necessary for nitrite to have protective effects by performing the same ischemia/reperfusion simulation in myoglobin deficient mice [43]. Surprisingly, myoglobin deficient mice are viable and show no obvious physiological phenotype [44]. As shown below in Figure 7, ischemia was simulated by ligating the left coronary artery for 30 minutes followed by 24 hours of reperfusion. Nitrite (48 nmol) was supplemented 5 minutes prior to the reperfusion period [43].

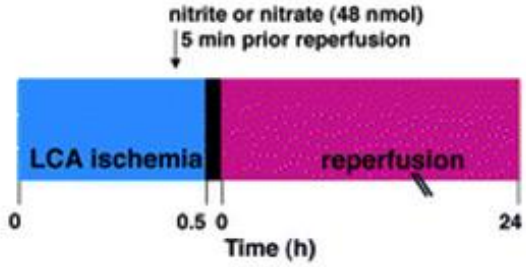

Figure 7. Procedure for *in vivo* ischemia/reperfusion simulation in the heart in a murine model. Ischemia was simulated by ligating the left coronary artery for 30 minutes followed by 24 hours of reperfusion. Nitrite was given 5 minutes before reperfusion [43].

Upon analysis of infarct size in the heart, they found that under control conditions, wild type (Mb+/+) and myoglobin deficient (Mb-/-) mice had no significant difference in infarct size. However, when nitrite was supplemented, it significantly reduced infarct size in Mb+/+ mice whereas it had no protective effects in Mb-/- mice (Figure 8) [43].

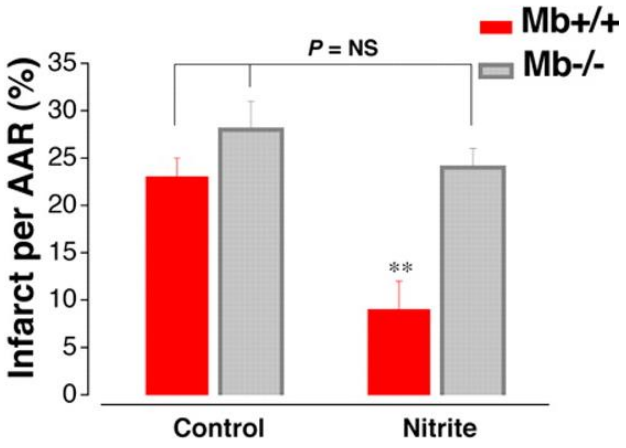

Figure 8. Nitrite significantly reduces infarct size in wild type (Mb+/+) but not myoglobin deficient (Mb-/-) mice after ischemia/reperfusion. Under control conditions, there is no significant difference between Mb+/+ and Mb-/- mice in infarct size. When nitrite is given, infarct size is significantly reduced in Mb+/+ mice but not Mb-/- mice [43].

Therefore, myoglobin is necessary for nitrite to mediate protection in ischemia/reperfusion. As previously described, myoglobin is a known regulator of mitochondrial function and notably, mitochondria are a central component to ischemia/reperfusion injury. During ischemia, oxygen is not available to be used as the final electron acceptor at complex IV of the electron transport chain, causing electrons to build up within the chain. Cells are then forced to generate ATP through glycolysis, which is a less efficient energy production method. ATP synthase (complex V) also begins to hydrolyze ATP in an attempt to maintain the membrane potential within the mitochondria; resulting in an overall reduction in ATP production [43, 46].

During reperfusion, when oxygen again becomes available, electrons rapidly re-enter the chain causing the electrons that had built up within the chain to leak out, resulting in ROS production. These ROS can subsequently oxidize proteins and lipids and cause DNA damage as well as cause cytochrome *c* release, causing in cell death [43, 46]. In 2007, Shiva et al. showed that treating isolated mitochondria with 20 μM nitrite significantly reduces ROS production after simulated ischemia/reperfusion (Figure 9) [42].

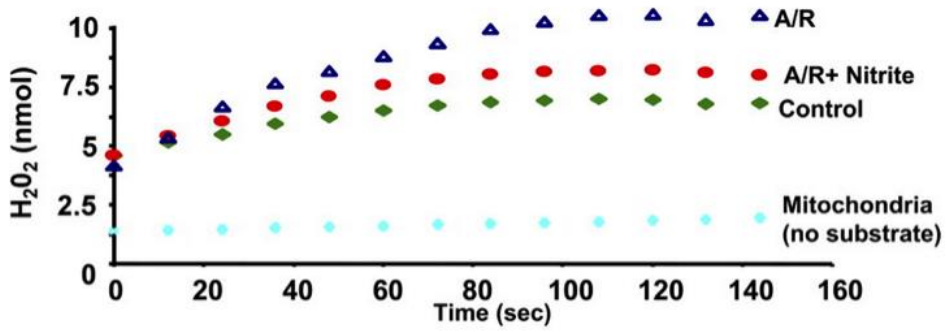

Figure 9. Nitrite treatment significantly reduces ROS production in isolated mitochondria after ischemia/reperfusion. Amplex Red measurement of ROS generation over time showed that after ischemia reperfusion, significant ROS are generated (blue dots). When treated with 20 μM nitrite (red dots), ROS production is reduced almost to that of control levels (green dots) [42].

This study also showed that treated isolated mitochondria with nitrite significantly increases mitochondrial protein S-nitrosation after an anoxic period (Figure 10, top). They further showed that this S-nitrosation specifically occurs at complex I of the electron transport chain (Figure 10, bottom) [42]. This S-nitrosation of complex I is likely responsible for reducing ROS production in ischemia/reperfusion.

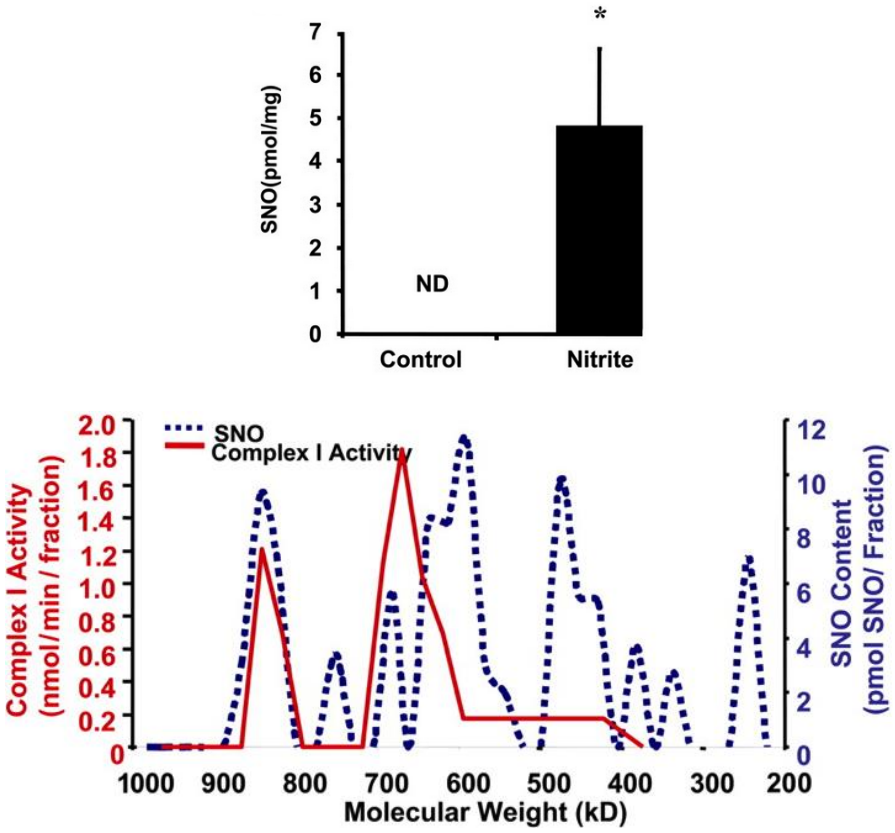

Figure 10. Nitrite treatment significantly increases complex I S-nitrosation. Treating isolated mitochondria with 480 nmol nitrite significantly increases mitochondrial protein S-nitrosation (top). Further analysis revealed this S-nitrosation occurs at complex I of the electron transport chain (bottom) [42].

More recently in 2013, Chouchani et al. showed that nitrite specifically S-nitrosates the ND3 subunit of complex I. As shown in Figure 11, during ischemia, complex I undergoes a conformational change, which causes a thiol group on the ND3 subunit to become exposed. Nitrite can then S-nitrosate this residue, inactivating complex I, thereby inhibiting electrons from entering the chain. This, in turn, inhibits ROS production during reperfusion. Furthermore, this post-translational modification is reversible, which allows complex I to be reduced to its original active form, thereby permitting respiration to continue as normal after reperfusion [47].

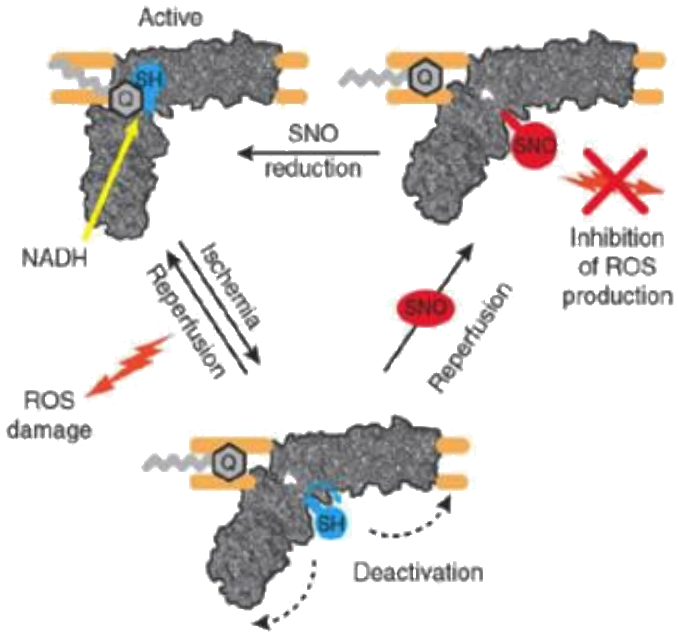

Figure 11. Nitrite S-nitrosates the ND3 subunit of complex I to inhibit ROS production during reperfusion. Nitrite S-nitrosates the ND3 subunit of complex I, resulting in its inactivation, which inhibits ROS production during reperfusion. Complex I can then be reduced and return to is active form [47].

As described, it is known that myoglobin as well as S-nitrosation of complex I are necessary for mitochondrial protection in ischemia/reperfusion injury. Therefore, the hypothesis for this aim is that myoglobin catalyzes the reduction of nitrite to nitric oxide to mediate complex I S-nitrosation in ischemia/reperfusion, thereby reducing cell death and tissue damage.

4.1.1 Stable transfection of human myoglobin in CHO cells

To determine the effect of myoglobin expression on nitrite-mediated protection in ischemia/reperfusion, the CHO cell line, which contains no endogenous myoglobin, was used. CHO cells were transfected with a vector (CHOR) or human myoglobin (CHOMb). A representative western blot in Figure 12 shows CHOR cells do not contain myoglobin and human myoglobin was successfully stably transfected in CHOMb cells.

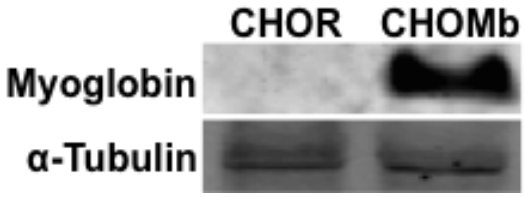

Figure 12. CHO cells were successfully transfected to stably express human myoglobin (CHOMb).

To verify that stable expression of human myoglobin does not cause any significant changes in overall morphology of CHO cells, bright field images were taken with a 10X objective of both cell lines. These images revealed that myoglobin expression does not cause any obvious morphological changes (Figure 13).

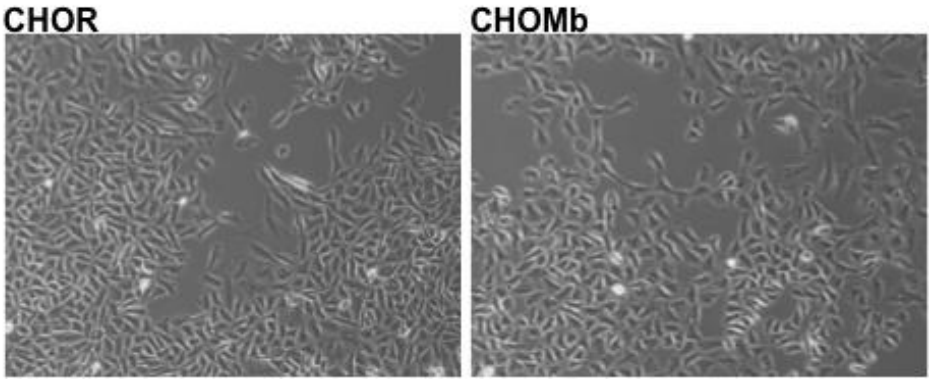

Figure 13. Stable transfection of myoglobin in CHO cells does not alter overall cell morphology. Bright field images show CHOR cells (left) transfected with an empty vector and CHOMb cells (right) transfected to stably express human myoglobin.

4.1.2 Nitrite treatment promotes cell survival after ischemia/reperfusion in CHOMb cells

To simulate ischemia/reperfusion injury *in vitro*, CHOR and CHOMb cells were subjected to hypoxia (1% O_2) for 2 hours followed by 2 hours of reoxygenation (20% O_2) with 5 μM nitrite supplemented before reoxygenation (Figure 14). At the completion of the reoxygenation period, cell death was quantified using the lactate dehydrogenase (LDH) release assay. When cells become damaged, LDH, which is responsible for the conversion of lactate to pyruvate, is released into the media. As shown in Figure 15, by measuring the rate at which NADH is oxidized to NAD^+, the amount of LDH can be determined, as they are directly correlated. Results are presented as the amount of LDH released into the media as a percent of total LDH, as shown in the equation below:

$$LDH\ (\%) = \frac{LDH_{media}}{LDH_{media} + LDH_{cell}}$$

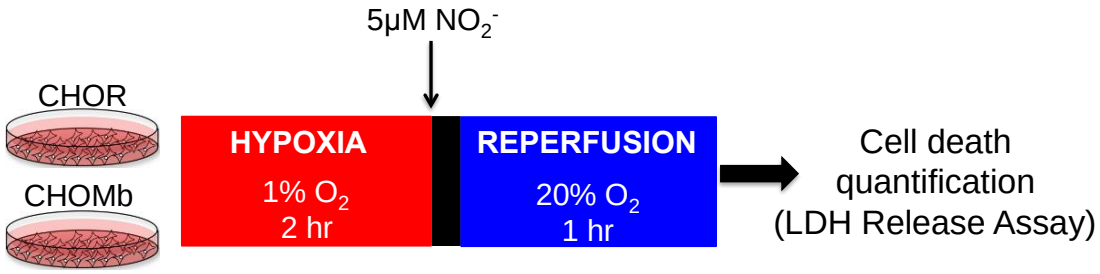

Figure 14. Procedure for simulating ischemia/reperfusion *in vitro*. CHOR and CHOMb cells were subjected to 1 hour of hypoxia (1% O_2) followed by 2 hours of reoxygenation (20% O_2) with 5 μM nitrite supplemented before reoxygenation. Cell death was then quantified by measuring LDH released into the cell media.

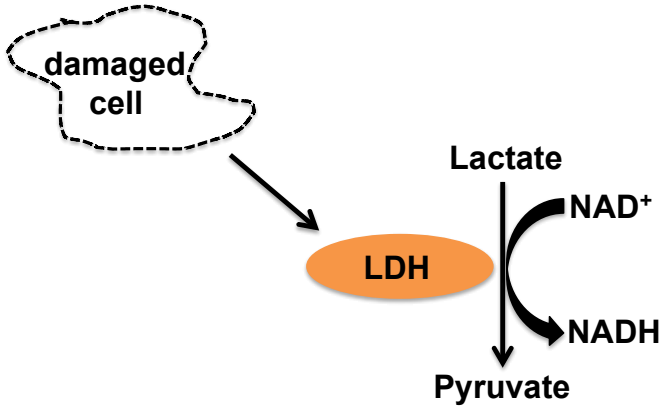

Figure 15. Rationale behind lactate dehydrogenase (LDH) release assay. The rate of NADH oxidized to NAD^+ is measured, which is directly correlated to the amount of LDH in the media.

As shown in Figure 16, after simulated ischemia/reperfusion with no nitrite treatment, CHOR and CHOMb cells experience the same amount of cell death. When 5 μM nitrite was supplemented, cell death was significantly reduced in CHOMb but not CHOR cells.

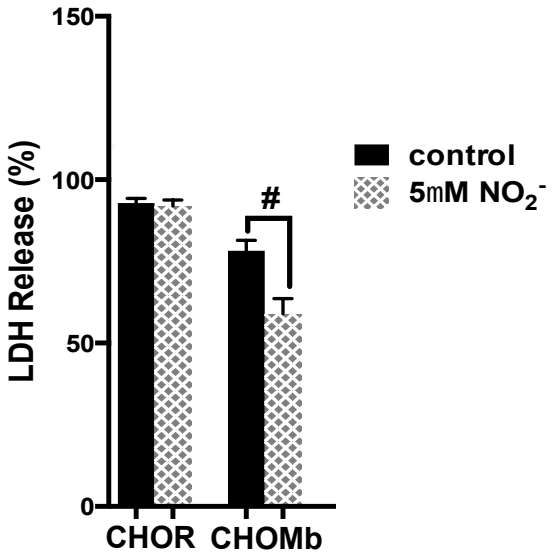

Figure 16. Nitrite significantly reduces cell death after ischemia/reperfusion injury in CHOMb cells. After ischemia/reperfusion, CHOR and CHOMb cells experience the same level of cell death under control conditions. When 5 μM nitrite is supplemented, cell death is significantly reduced in CHOMb but not CHOR cells. Data are represented as LDH in the media as a percent of total LDH. Data are represented as mean ± SEM. (# $p<0.05$).

4.1.3 Treating CHOR and CHOMb cells with nitrite increases protein S-nitrosation in CHOMb but not CHOR cells

To show that myoglobin catalyzes the reduction of nitrite to nitric oxide, which can subsequently S-nitrosate proteins within the cell, the level of protein S-nitrosation was measured in the whole cell and mitochondria. Shown in Figure 17, treating CHOR and CHOMb cells with nitrite significantly increased protein S-nitrosation in both whole cell and the mitochondria in CHOMb but not CHOR cells. This suggests myoglobin expression is required to reduce nitrite to nitric oxide, which can subsequently S-nitrosate proteins within the cell.

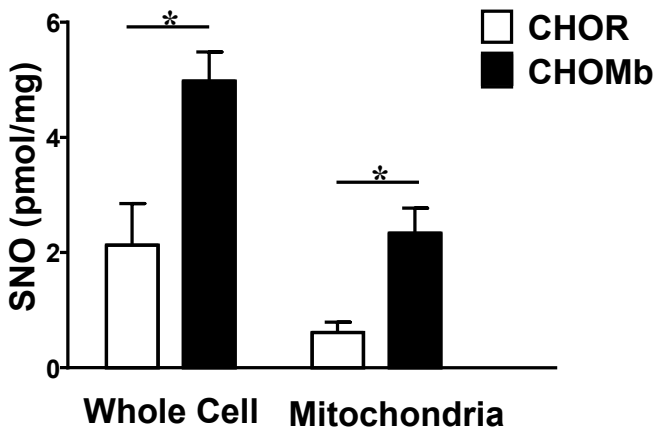

Figure 17. Protein S-nitrosation in the whole cell and mitochondria in CHOR and CHOMb cells after nitrite treatment. Nitrite treatment increases S-nitrosation levels in the whole cell and mitochondria of CHOMb but not CHOR cells. (* $p<0.01$)

4.1.4 Myoglobin-dependent nitrite-mediated protection occurs through mitochondrial complex I

To determine whether myoglobin and nitrite are mediating protection after ischemia/reperfusion through complex I, complex I was knocked down in CHOR and CHOMb cells and subjected to ischemia/reperfusion *in vitro.* Complex I was knocked down by transfecting cells with NDUFAF1 (NADH dehydrogenase assembly factor 1) siRNA. NDUFAF1 is a protein required for proper complex I assembly; therefore, by silencing NDUFAF1, complex I is effectively knocked down. As a control, CHOR and CHOMb cells were also transfected with non-targeted siRNA. As shown in Figure 18, after transfections, cells were exposed to the same hypoxia/reoxygenation protocol previous described and cell death quantified by LDH release.

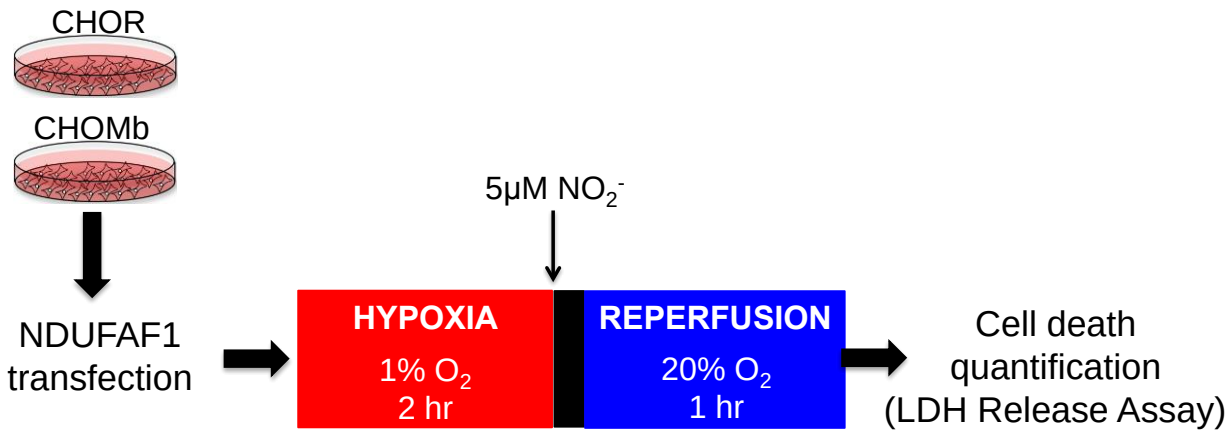

Figure 18. Procedure for transfecting CHOR an CHOMb cells and simulation of ischemia/reperfusion *in vitro.* CHOR and CHOMb cells were transfected with control or NDUFAF1 siRNA and subjected to 1 hour of hypoxia (1% O_2) followed by 2 hours of reoxygenation (20% O_2) with 5 μM nitrite supplemented before reoxygenation. Cell death was then quantified by measuring LDH released into the media.

As shown in Figure 19, when transfected with control siRNA, nitrite significantly reduces cell death in CHOMb cells but not CHOR cells, consistent with the results obtained when no transfection was performed. When transfected with NDUFAF1 siRNA, nitrite still does not provide protection in CHOR cells and the protection previously observed with nitrite treatment in CHOMb cells is eliminated. Therefore, myoglobin-dependent nitrite-mediated protection occurs through complex I.

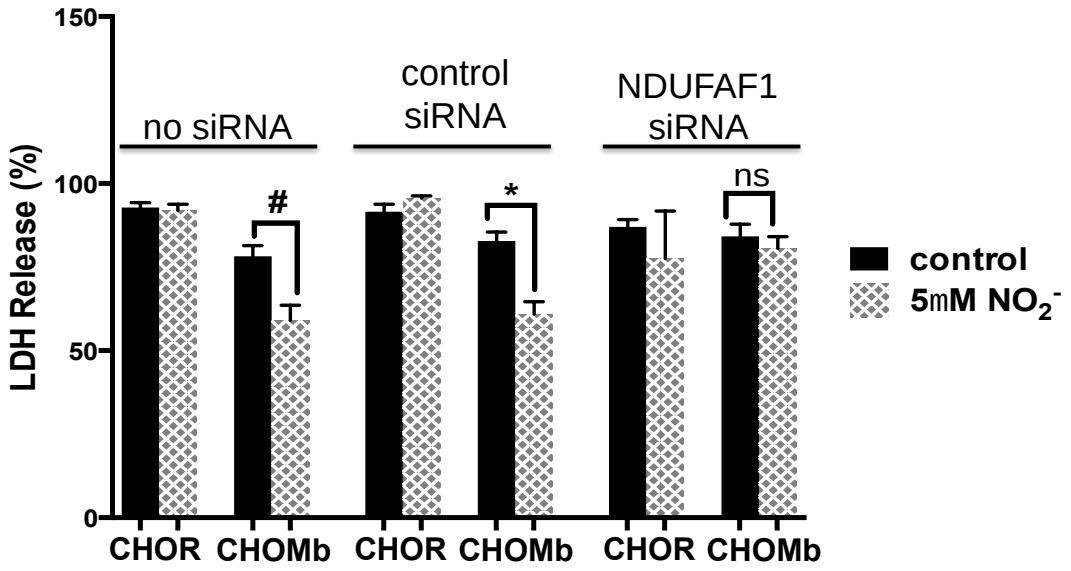

Figure 19. Silencing complex I eliminates nitrite's protective effects in CHOMb cells. When transfected with control siRNA, nitrite significantly reduces cell death in CHOMb but not CHOR cells. When transfected with NDUFAF1 siRNA, the protection previously mediated by nitrite in CHOMb cells is eliminated. Two-way ANOVA with Bonferroni correct was used to determine significance. Data are presented as mean ± SEM. (# $p<0.05$; * $p<0.01$)

As shown in the pathway in Figure 20, the findings presented in this aim show that myoglobin catalyzes the reduction of nitrite to nitric oxide, which can subsequently S-nitrosate complex I to inhibit ROS production during reperfusion. By reducing ROS production, cell death is reduced, thereby promoting cell survival and mitigating tissue damage.

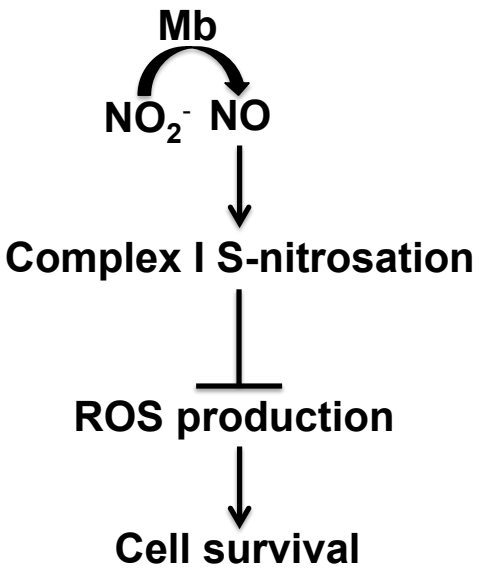

Figure 20. Myoglobin mediates cell survival through reduction of nitrite to nitric oxide to S-nitrosate complex I and inhibit ROS production.

4.2 AIM 2

As previously described, myoglobin is known for its expression in rapidly respiring cells, specifically cardiac and skeletal muscle cells where it is expressed in very high concentrations [16, 18]. However, myoglobin is now recognized for its expression in other cell types, including cancer tumors [22-24]. Myoglobin was first discovered by accidental staining in several human carcinomas in 2001. Since this initial discovery, myoglobin has been found it be expressed in several cancers of epithelial origin, including breast, ovary, colon and lung cancer [22].

In 2010, Kristiansen et al. found that myoglobin expression is associated with better patient prognosis. As shown in the ten-year Kaplan-Meyer curve in Figure 21, patients with myoglobin positive tumors (Mb+) have significantly better survival than those with myoglobin negative tumors (Mb-) [22]. Notably, however, it is still unknown what myoglobin is doing in these tissues to improve patient outcomes. Therefore, the hypothesis for this aim is that myoglobin causes a reduction in cell proliferation in breast cancer cells through modulation of mitochondrial function and dynamics.

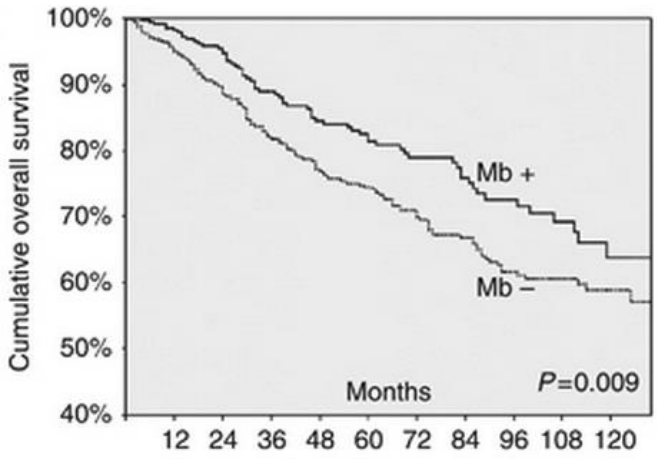

Figure 21. Patients with myoglobin positive tumors (Mb+) have significantly better survival than patients with myoglobin negative (Mb-) tumors [22].

4.2.1 Stable transfection of human myoglobin in MDA-MB-231 cells

To determine how myoglobin affects proliferation of breast cancer cells, the breast cancer cell line MDA-MB-231, which contains no endogenous myoglobin, was utilized. These cells were transfected to stably express human myoglobin (231Mb). A representative western blot in Figure 22 shows control MDA-MB-231 cells (231) do not contain myoglobin and 231Mb cells were successfully transfected to stably express human myoglobin.

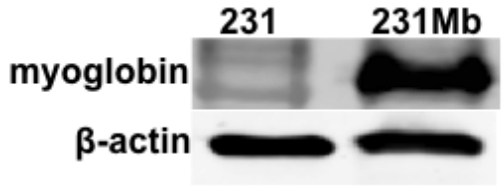

Figure 22. 231 cells were successfully transfected to stably express human myoglobin (231Mb).

To verify that stable expression of human myoglobin does not cause any significant changes in overall morphology of 231 cells, bright field images were taken with a 10X objective of both cell lines. These images revealed that myoglobin expression does not cause any obvious morphological changes (Figure 23).

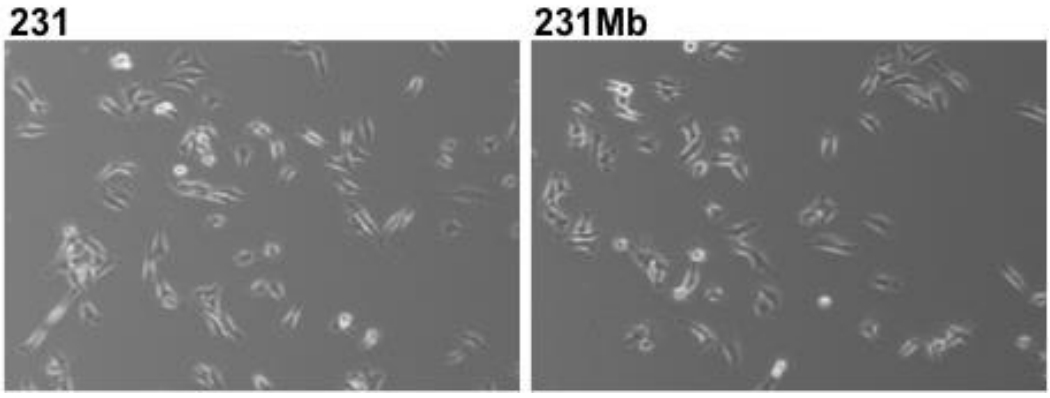

Figure 23. Stable transfection of myoglobin in 231 cells does not alter overall cell morphology. Bright field images show 231 control cells (left) and 231Mb cells (right) transfected to stably express human myoglobin.

4.2.2 Myoglobin expression decreases proliferation and migration of MDA-MB-231 cells

To begin investigating the function of myoglobin in breast cancer cells, the proliferation of 231 and 231Mb cells was first analyzed. As shown in Figure 24, 24-hour ^{3}H thymidine incorporation showed that 231Mb cells have significantly lower proliferation compared to 231 control cells ($p<0.01$). Additionally, cell migration was analyzed by a 24-hour scratch assay. The percentage scratch closure was determined to quantify the migratory capability of the cells. 231Mb cells showed significantly less migration compared to 231 control cells ($p<0.05$). Representative images taken at 0 and 24 hours are shown in Figure 25 A with quantification in Figure 25 B.

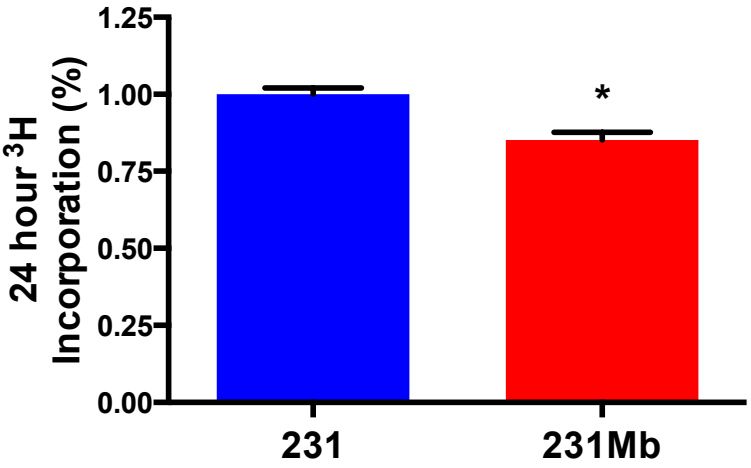

Figure 24. 231Mb cells proliferate significantly less than 231 control cells measured by 24-hour ^{3}H thymidine incorporation. 231 proliferation rates are normalized to 1.00 and 231Mb rates represented as a percentage of 231. Data are presented as mean ± SEM. (* $p<0.01$).

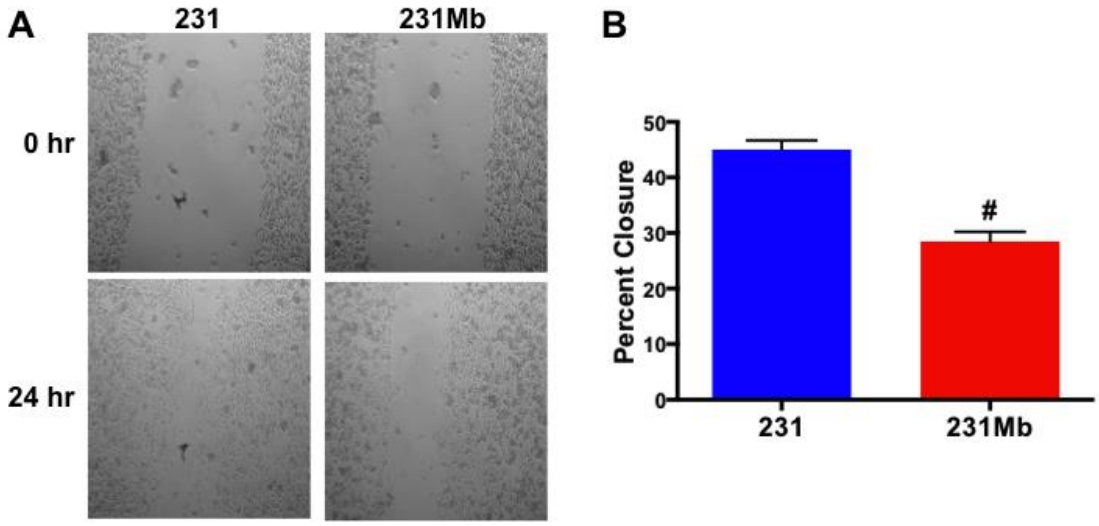

Figure 25. Myoglobin expression significantly reduces cell migration. Cell migration was measured by a 24-hour scratch assay with the percent scratch closure calculated at the 24-hour time point. Representative images are shown in A and quantification shown in B. Data are presented as mean ± SEM. (# $p<0.05$).

4.2.3 Myoglobin expression does not increase apoptosis

Lower ^{3}H thymidine incorporation could be due to either less proliferation or more apoptosis. To be sure the lower ^{3}H thymidine incorporation observed in the 231Mb cells was due to less proliferation, apoptosis was measured by annexin V staining and flow cytometry analysis. As shown in Figure 26, 231 and 231Mb cells do not have significantly different annexin V positive cells ($p=0.2$).

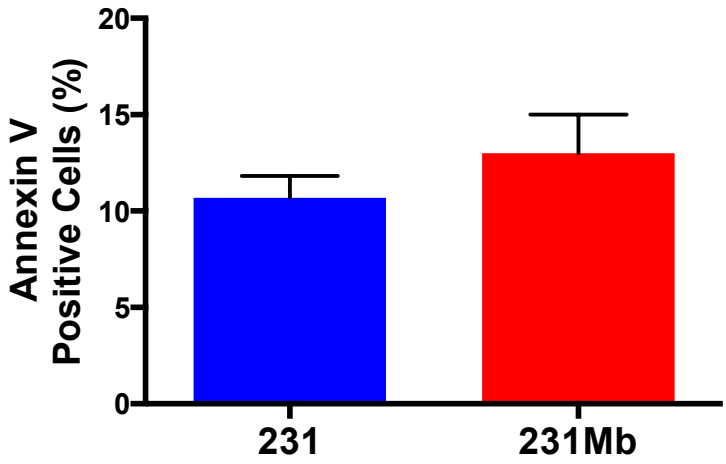

Figure 26. Myoglobin expression does not increase apoptosis. Flow cytometry analysis of annexin V staining shows no significant difference between 231 and 231Mb cells. Data are presented as mean ± SEM. (p=0.2)

4.2.4 Myoglobin expression in 231 cells is associated with mitochondrial fusion

Because there is a significant difference in proliferation and migration of 231 and 231Mb cells and a significant amount of ATP is necessary to support these processes, myoglobin's effect on mitochondria was investigated. First, the overall morphology of mitochondria in 231 and 231Mb cells was examined. Immunofluorescence staining of TOM20, a protein localized to the outer mitochondrial membrane, showed that 231 control cells have small, fragmented mitochondria (Figure 27A) while 231Mb cells have large networks of fused mitochondria (Figure 27B).

Mitochondria morphology was also analyzed by electron microscopy at 15,000X. Consistent with TOM20 staining, electron microscopy analysis showed 231 cells have fragmented mitochondria while 231Mb cells have fused mitochondria. Representative images are shown in Figure 28A. The extent of mitochondrial fusion was determined by calculating mitochondria interconnectivity, which can be quantified as area to perimeter ratio. This quantification showed 231Mb cells have significantly greater mitochondria interconnectivity compared to 231 control cells, shown in Figure 28B.

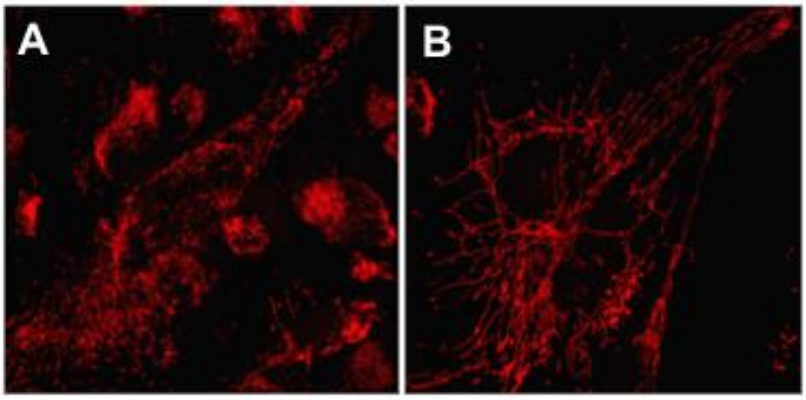

Figure 27. 231Mb cells have significant mitochondrial fusion. TOM20 staining of the outer mitochondrial membrane of 231 (A) and 231Mb (B) cells shows 231 cells have small, fragmented mitochondria whereas 231Mb cells have fused mitochondria.

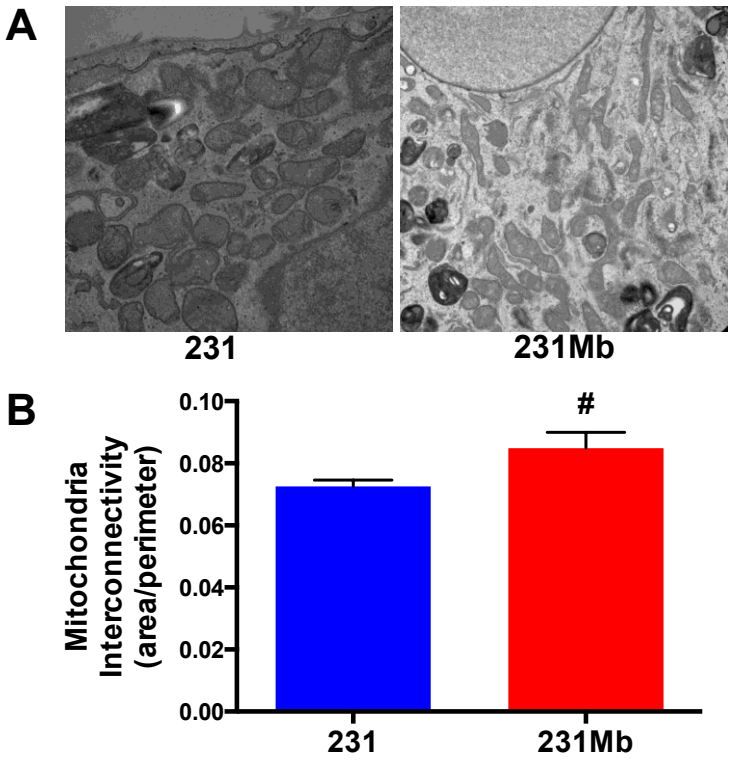

Figure 28. 231Mb cells show significantly greater mitochondria interconnectivity by electron microscopy. Representative electron microscopy images of mitochondria of 231 and 231Mb (A) cells imaged at 15,000X and ImageJ quantification (B) show 231 control cells have small, fragmented mitochondria while 231Mb cells have fused, elongated mitochondria. Mitochondria interconnectivity is presented as mean ± SEM. (# $p<0.05$).

4.2.5 Mitochondrial fusion in 231Mb cells is due to upregulation of mfn1 & 2 and downregulation of drp1

As previously described, mitochondria are very dynamic structures, constantly coming together through the process of fusion and breaking apart during fission. The mitofusin proteins (mfn 1 & 2) are responsible for mediating fusion while dynamin related protein-1 (drp1) is responsible for mediating fission [8, 9].

The expression of mitochondrial fission (drp1) and fusion (mfn1 &2) proteins was analyzed to determine whether altered expression of these proteins was responsible for the fusion observed in the 231Mb cells. As shown in Figure 29, western blot and densitometry analysis of these proteins revealed that 231Mb cells have significantly greater expression of the fusion proteins mfn1 and a strong trend for increased expression of mfn2. Furthermore, 231Mb cells have significantly lower expression of the fission protein drp1. This suggests myoglobin is driving mitochondrial fusion by increasing mfn1 expression and decreasing drp1 expression.

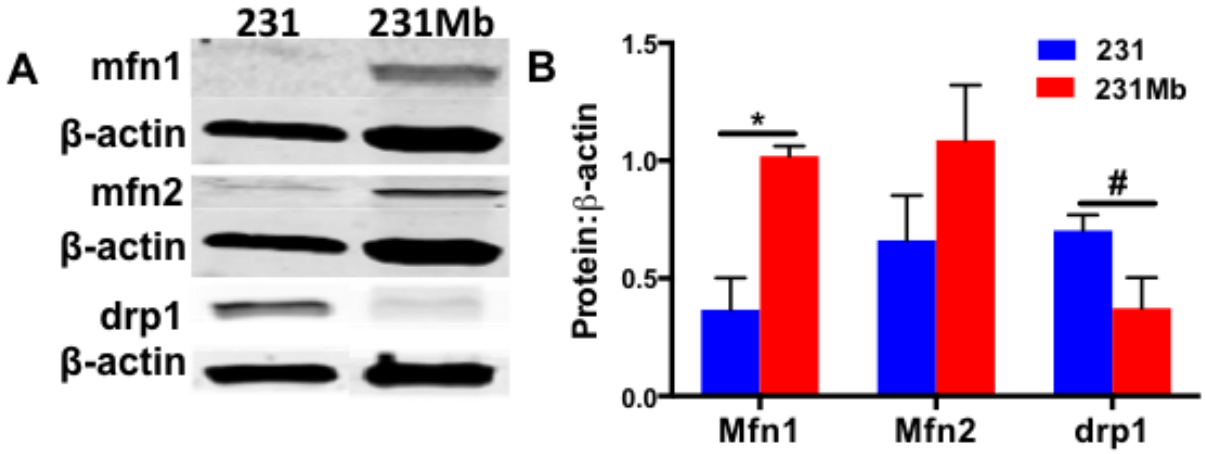

Figure 29. Mfn 1 & 2 are upregulated and drp1 downregulated in 231Mb cells. Western blot and densitometry quantification shows 231Mb cells have significantly greater mfn1 expression (* $p<0.01$), a strong trend for increased mfn2 expression, and significantly lower expression of drp1 (# $p<0.05$) than 231 control cells. Protein expression is normalized to β-actin expression and represented as mean ± SEM.

4.2.6 Myoglobin expression is responsible for reduced proliferation in 231Mb cells

Thus far, it has been shown that myoglobin expression is associated with a reduction in proliferation.

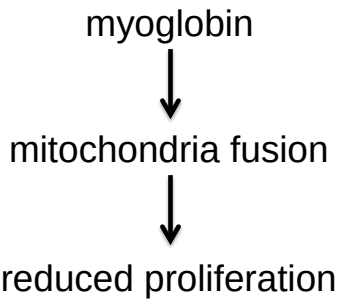

Figure 30. Myoglobin expression is associated with mitochondrial fusion and reduced cell proliferation.

To investigate whether myoglobin expression is responsible for causing decreased proliferation in 231Mb cells, myoglobin was knocked-down by siRNA transfection in 231 and 231Mb cells and the proliferation analyzed over 24 hours by crystal violet staining. When transfected with non-targeted control siRNA, 231Mb cells proliferate significantly less than 231Mb cells. Silencing myoglobin in 231 control cells had no effect on proliferation, which would be expected, as these cells do not contain any myoglobin. However, silencing myoglobin in 231Mb cells resulted in a significant increase in proliferation, with proliferation rates restored to the level of 231 control cells (Figure 31).

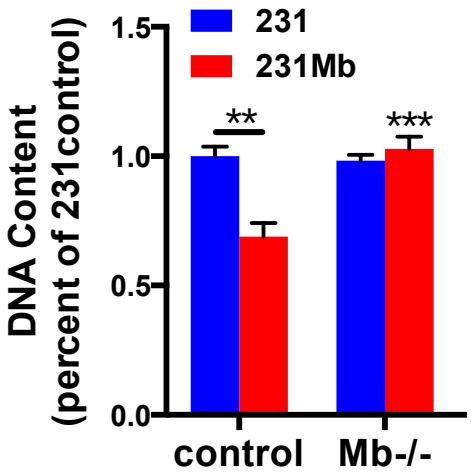

Figure 31. Silencing myoglobin by siRNA transfection in 231Mb cells restores proliferation. When 231 and 231Mb cells are transfected with control siRNA, 231Mb cells proliferate significantly less than 231 control cells (** $p<0.001$). When myoglobin is silenced, proliferation is restored in 231Mb cells (*** $p<0.0001$). Proliferation rates are normalized to 231 and represented as a percent of 231 control group. Data are presented as mean ± SEM.

4.2.7 Mitochondrial fusion is responsible for reduced proliferation in 231Mb cells

To determine whether mitochondrial fusion is also responsible for lower proliferation in 231Mb cells, the mitochondrial fusion proteins mfn1 and mfn2 were silenced by siRNA transfection in 231 and 231Mb cells. Upon transfection of either mfn1 or mfn2 in 231 cells, proliferation increased slightly, as these cells do not have extensively fused mitochondria and thus silencing the fusion proteins would not have made a significant impact on the mitochondria. However, silencing either mfn1 or mfn2 in the 231Mb cells resulted in a significant increase in proliferation, restoring proliferation to that of 231 control levels (Figure 32). These findings suggest that in addition to myoglobin, mitochondrial fusion is also a driving force of the decreased proliferation.

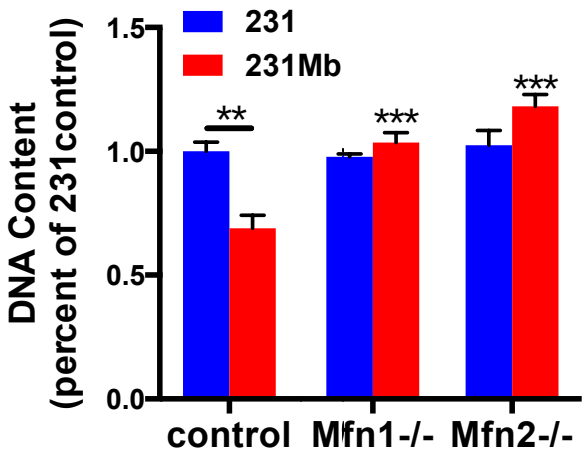

Figure 32. Silencing mfn 1 & 2 by siRNA transfection restores proliferation of 231Mb cells. When 231 and 231Mb cells are transfected with control siRNA, 231Mb cells proliferate significantly less than 231 control cells (** $p<0.001$). When mfn 1 & 2 are silenced, proliferation is restored in 231Mb cells (*** $p<0.0001$). Proliferation rates are normalized to 231 and represented as a percent of 231 control group. Two-way ANOVA with a Bonferroni correction was used to determine significance. Data are presented as mean ± SEM.

4.2.8 Myoglobin expression causes cell cycle arrest at the G1/S phase transition of the cell cycle

The mitochondrial phenotype observed in 231 and 231Mb cells was an interesting finding, as mitochondrial dynamics regulate the cell cycle. As shown by Lippincott-Schwartz et al. in 2009 and Yamano and Youle in 2011, proliferating cells as well as cells progressing from the G2 to M phase of the cell cycle have punctate, fragmented mitochondria whereas cells progressing from G1 to S phase have fused, elongated mitochondria (Figure 33) [48, 49]. Lippincott-Schwartz et al. further showed that mitochondria can become hyperfused at the G1/S phase transition, which causes cell cycle arrest.

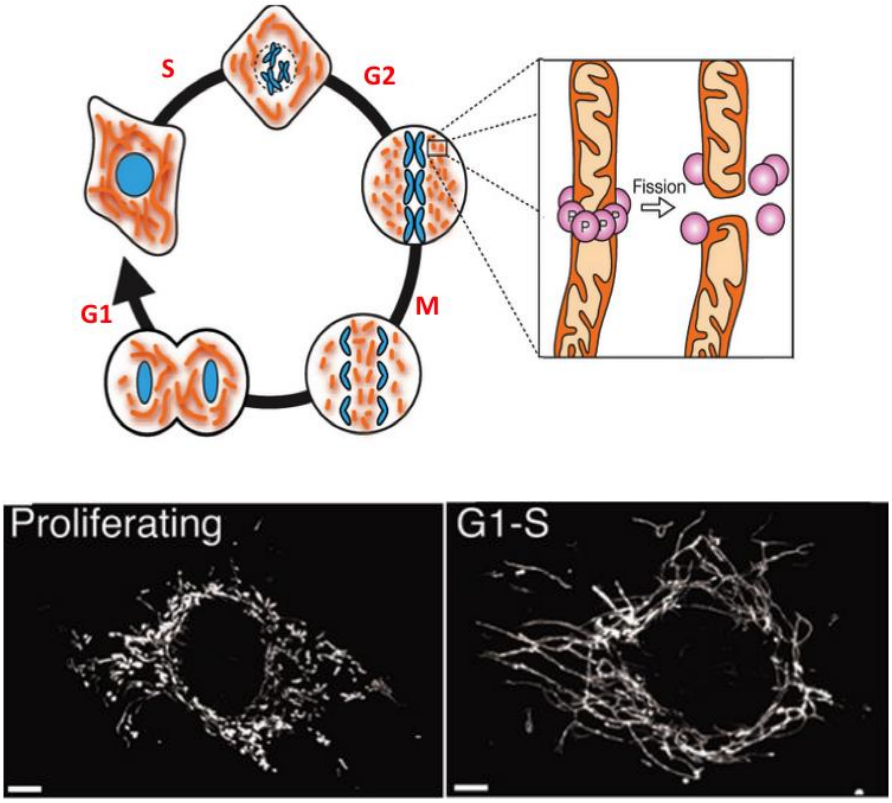

Figure 33. Cells progressing from G2 to M phase of the cell cycle have fragmented mitochondria and cells progressing G1 to S phase have elongated, fused mitochondria [48, 49].

This is particularly interesting, as the mitochondrial phenotypes of 231 and 231Mb cells is exactly that of proliferating cells and cells going through the G1/S phase transition, respectively. To determine whether the excessive mitochondrial fusion in 231Mb cells causes cell cycle arrest at the G1/S phase transition, the expression of cyclin E and p21 were analyzed. Cyclin E and p21 are proteins that regulate cell cycle progression specifically as cell progress from G1 to S phase. Cyclin E is necessary for cells to pass into S phase whereas p21 is causes growth arrest at this transition and is also a mediator of cellular senescence.

Western blot analysis of cyclin E and p21 in 231 and 231Mb cells revealed that 231Mb cells have significantly lower cyclin E expression and significantly greater p21 expression than 231 control cells (Figure 34). These results suggest that 231Mb cells are unable to pass from G1 to S phase and thus experience cell cycle arrest at this transition. Therefore, as shown in the schematic in Figure 35, myoglobin expression causes mitochondrial hyperfusion to cause cell cycle arrest and reduce proliferation.

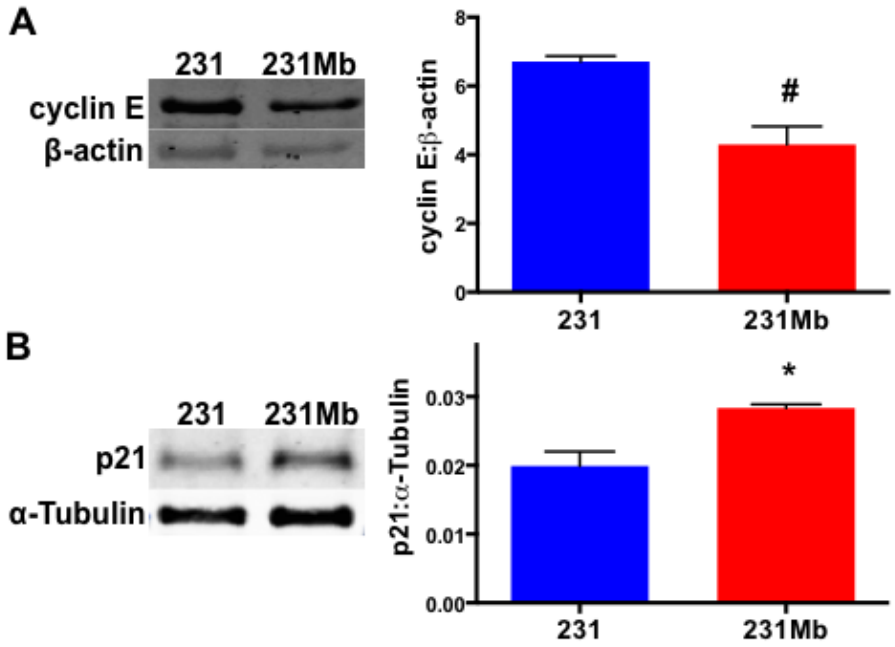

Figure 34. 231Mb cells have significantly lower cyclin E expression and significantly greater p21 expression. Densitometry analysis of cyclin E and p21 expression levels show 231Mb cells have significantly lower cyclin E expression (A) and significantly higher p21 expression (B). Protein expression is normalized to β-actin or α-Tubulin expression and represented as mean ± SEM. (# $p<0.05$; * $p<0.01$)

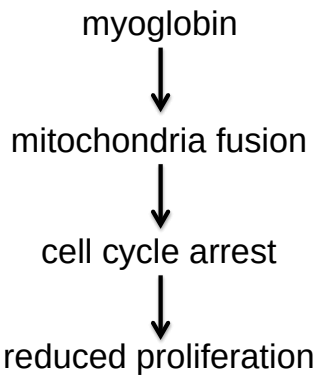

Figure 35. Myoglobin expression is associated with mitochondrial fusion, which causes cell cycle arrest and reduces cell proliferation.

4.2.9 Myoglobin-expressing tumors have lower end-tumor volume and weight than control tumors

While all *in vitro* experiments showed that myoglobin expression and mitochondrial fusion drive a decrease in proliferation in breast cancer cells, it was unknown whether this mechanism was relevant in a model of cancer *in vivo*. To test this, 5 scid mice were injected in both mammary fat pads with 3×10^6 231 control cells or 231Mb cells. Tumors were allowed to grow until tumors of the control group reached a volume of $1.5cm^3$, when animals were sacrificed and final tumor volume and weight analyzed. Consistent with the *in vitro* proliferation results, the myoglobin-expressing tumors showed a strong trend for lower tumor volume (Figure 36A) and weight (Figure 36B) compared to control tumors.

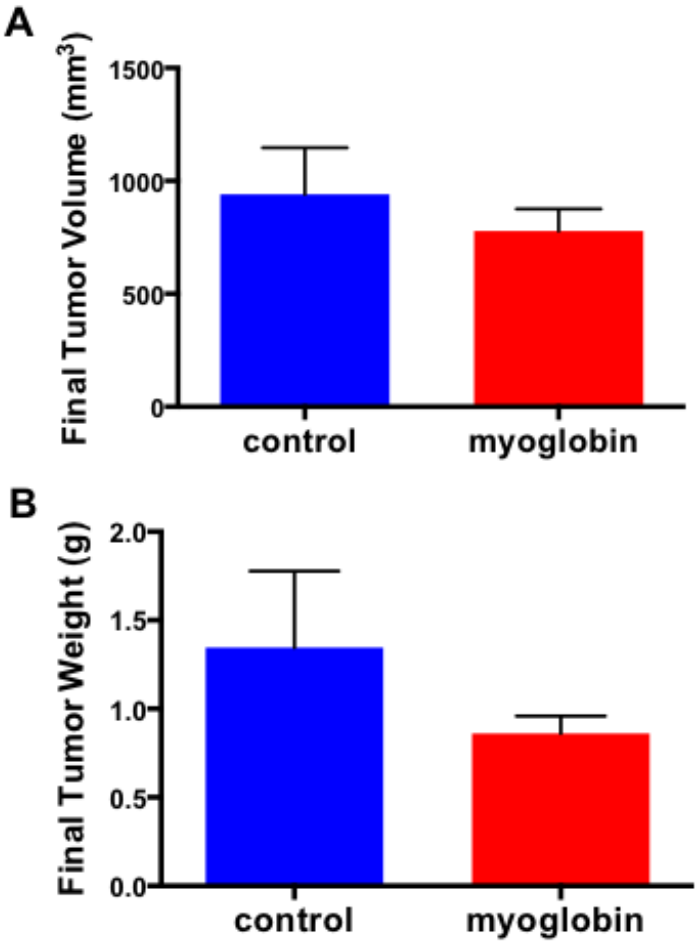

Figure 36. Myoglobin-expressing tumors show a strong trend for reduced end tumor volume and weight. N=5 mice per group. Data are presented as mean ± SEM.

4.2.10 Myoglobin-expressing tumors have a fused mitochondrial phenotype

Because the mitochondrial phenotype in 231 control and 231Mb cells were drastically different, to determine whether the same changes in the myoglobin cells also occur *in vivo,* the mitochondrial morphology of the tumors was also analyzed by electron microscopy. These results showed that myoglobin-expressing tumors have elongated, fused mitochondria while the

control tumors have punctate, fragmented mitochondria, shown in Figure 37A. The extent of mitochondrial fusion was quantified by area/perimeter ratio, with myoglobin-containing tumors having significantly greater interconnectivity ($p<0.05$) (Figure 37B).

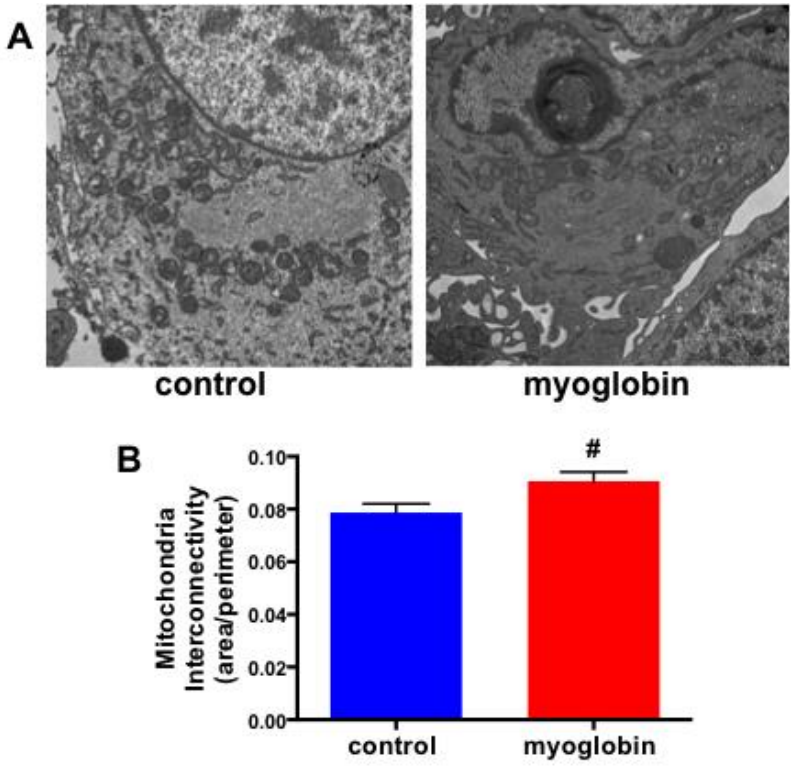

Figure 37. Myoglobin-expressing tumors have fused mitochondria. Electron microscopy analysis of tumor tissue show that myoglobin-expressing tumors have elongated, fused mitochondria whereas control tumors have punctate, fragmented mitochondria (A). Mitochondria interconnectivity was quantified by the ratio of area to perimeter, with myoglobin tumors having significantly greater mitochondrial interconnectivity. Data are expressed as mean ± SEM. (#$p<0.05$).

4.2.11 Myoglobin-expressing tumors show cell cycle arrest at the G1/S phase transition

Since myoglobin-expressing tumors showed a trend for reduced proliferation and fused mitochondria, consistent with what was observed in 231Mb cells *in vitro*, it was hypothesized that the tumor cells may also be experiencing cell cycle arrest at the G1 to S phase transition. Thus, cyclin E and p21 expression levels were analyzed in the tumor tissue. Western blot analysis results showed that myoglobin-expressing tumors have significantly lower expression of cyclin E ($p<0.05$) and significantly greater p21 expression ($p<0.05$) compared to control tumors. Western blot images and densitometry quantification for cyclin E and p21 are shown in Figure 38A and B, respectively. These findings suggest myoglobin-expressing tumors may be experiencing cell cycle arrest, consistent with the *in vitro* analysis of 231Mb cells.

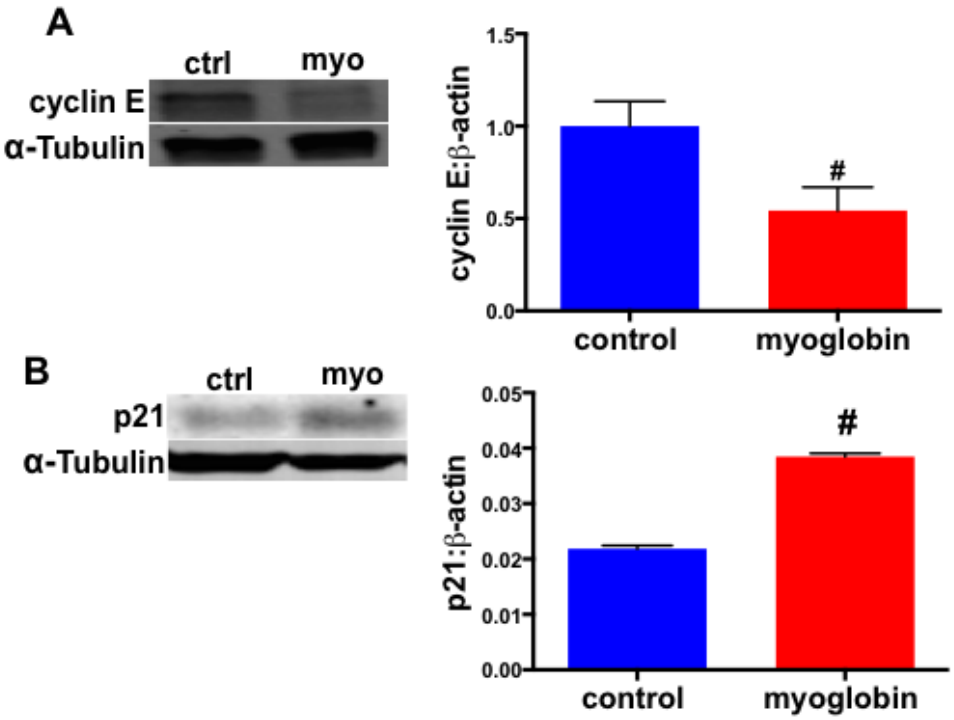

Figure 38. Myoglobin-expressing tumors have significantly lower cyclin E expression and significantly greater p21 expression. Western blot analysis of cyclin E is shown in A and p21 in B. Protein expression is normalized to α-Tubulin expression and represented as mean ± SEM. (# $p<0.05$)

4.2.12 231Mb cells and myoglobin-expressing tumors have decreased parkin expression

Thus far, the results presented show that myoglobin expression is associated with mitochondrial hyperfusion, which causes cell cycle arrest and reduces cell proliferation (Figure 35). However, it is still unknown how myoglobin causes mitochondrial fusion.

One protein of interest is parkin, which is an E3 ubuqitin ligase protein. Parkin is responsible for transferring ubiquitin to mitofusins on the outer mitochondrial membrane, thereby causing them to be degraded and preventing mitochondrial fusion, hence promoting mitochondrial fragmentation (Figure 39) [50, 51].

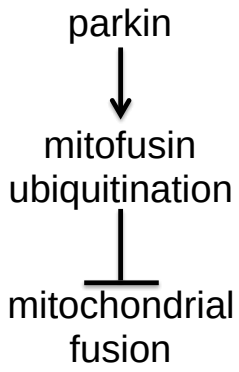

Figure 39. Parkin causes mitofusin ubiquitination, thereby inhibiting mitochondrial fusion.

To determine whether this was the mechanism by which fusion occurs in myoglobin-expressing cells and tumors, western blot analysis was done to assess parkin expression levels. Western blot analysis and densitometry quantification shown in Figure 40A of 231 and 231Mb cells showed that 231Mb cells have significantly lower expression of parkin compared to 231 control cells. Similarly, myoglobin-expressing tumors also have significantly lower parkin

expression than control tumors (Figure 40B). Therefore, myoglobin expression reduces parkin expression, which inhibits mitofusin ubiquitination to cause mitochondrial hyperfusion (Figure 41).

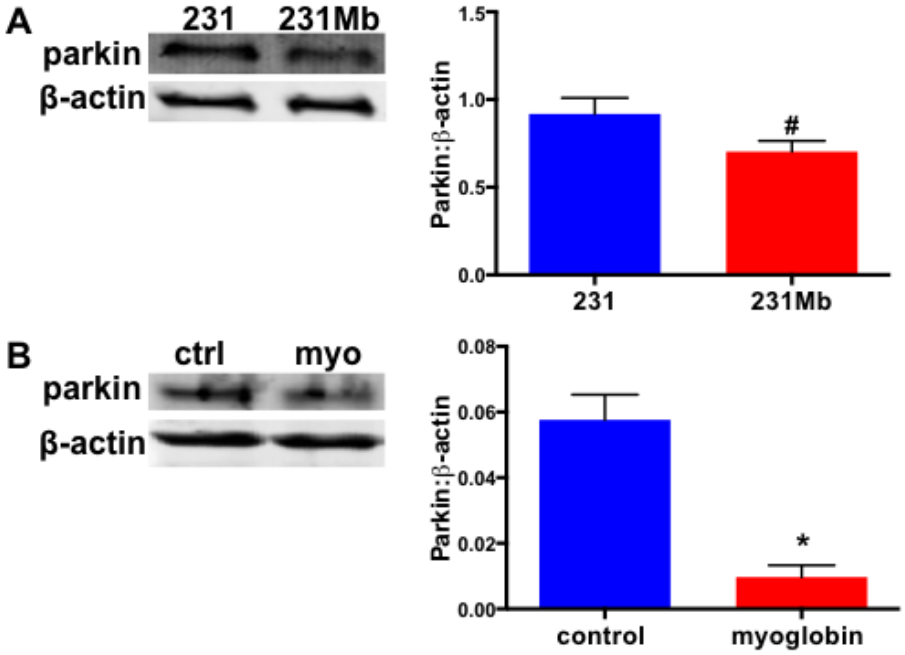

Figure 40. 231Mb cells and myoglobin-expressing tumors have significantly lower parkin expression and control cells and tissue. Protein expression is normalized to β-actin expression and represented as mean ± SEM. (# $p<0.05$; * $p<0.01$).

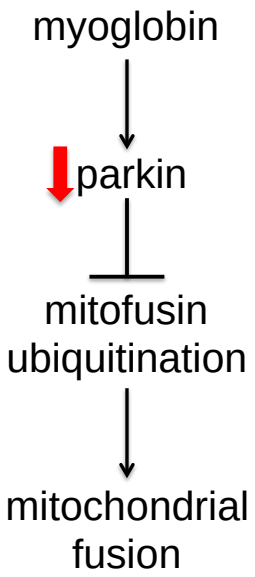

Figure 41. Myoglobin could cause a reduction in parkin expression to inhibit mitofusin ubiquitination and drive mitochondrial fusion.

4.2.13 Myoglobin expression reduces mitofusin ubiquitination

It has been shown that myoglobin causes a reduction in parkin expression. To determine whether this reduction in parkin results in a reduction of mitofusin ubiquitination to drive mitochondrial fusion, mfn1 was immunoprecipitated in 231 and 231Mb cells and ubiquitination determined by western blot. These results show that 231Mb cells have significantly less ubiquitination of mfn1 than 231 control cells (Figure 42) ($p<0.05$).

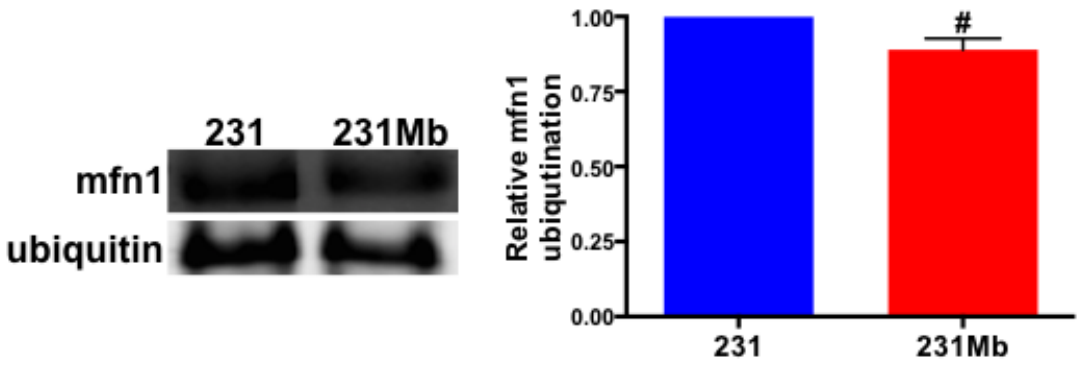

Figure 42. 231Mb cells have less mfn1 ubiquitination than 231 control cells. Western blot and densitometry analysis show mfn1 is ubiquitinated less in 231Mb cells than in 231 cells. Ubiquitin levels are normalized to mfn1 expression in each cell type. Data are presented as mean ± SEM. (# $p<0.05$).

As shown in the proposed pathway in Figure 43, the results presented here show that myoglobin expression causes a reduction in parkin expression, which reduces mfn1 ubiquitination. With reduced mfn1 ubiquitination, mfn1 will not be degraded, thereby resulting in mitochondrial hyperfusion. As described, mitochondrial hyperfusion causes cell cycle arrest at the G1/S transition of the cell cycle, thereby causing a reduction in cell proliferation and tumor growth.

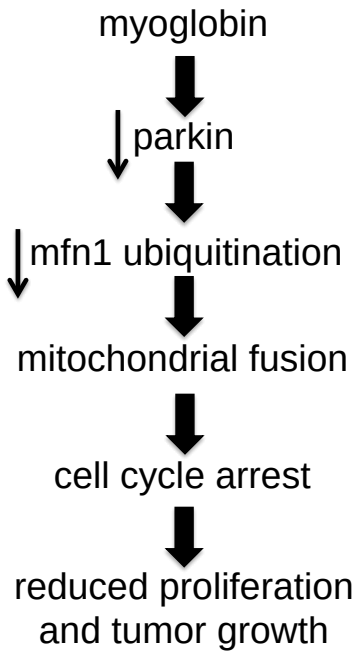

Figure 43. Myoglobin expression causes a reduction parkin expression to decrease mfn1 ubiquitination and drive mitochondrial fusion to cause cell cycle arrest and reduce cell proliferation.

4.2.14 231Mb cells have cytosolic but not mitochondrial ROS

One way in which parkin expression could be reduced is through its inactivation by oxidation. Notably, myoglobin is able to catalyze ROS production in the cytosol of the cell through its reaction with H_2O_2 [52].

$$Fe^{2+} + H_2O_2 \rightarrow Fe^{4+} \rightarrow Fe^{3+} + OH\bullet + OH^-$$

To determine whether myoglobin expression causes an altered intracellular oxidative state in 231Mb cells, mitochondrial and cytosolic ROS production was measured in 231 control and 231Mb cells. Mitochondrial-produced ROS was measured by the MitoSOX™ Red assay, which measures mitochondrial superoxide. There was no difference in superoxide produced between 231 control and 231Mb cells, as shown in Figure 44 ($p=0.5$).

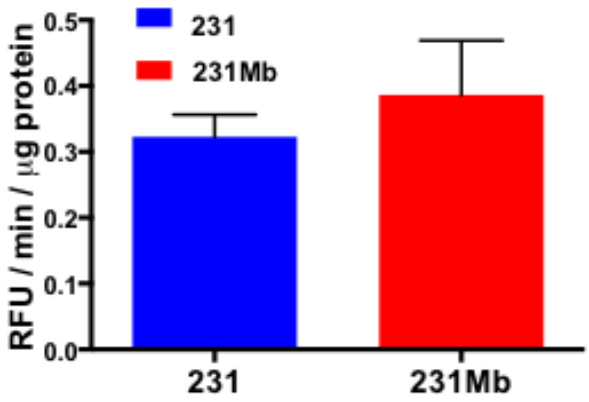

Figure 44. Myoglobin expression does not change amount of mitochondrial-produced ROS. As measured by the MitoSOX™ Red assay, there is no significant difference in mitochondrially-produced ROS in 231 and 231Mb cells. (p=0.5)

Cytosolic hydrogen peroxide generation was measured by the Amplex® Red assay. Cells were also treated with 0, 250, or 500nM mitoTEMPOL to scavenge mitochondrial ROS. Upon treatment of 231 cells with mitoTEMPOL, H_2O_2 production decreases, suggesting some of this ROS is originating from mitochondria. However, in 231Mb cells, treatment with mitoTEMPOL does not affect H_2O_2 production. These results are shown in Figure 45.

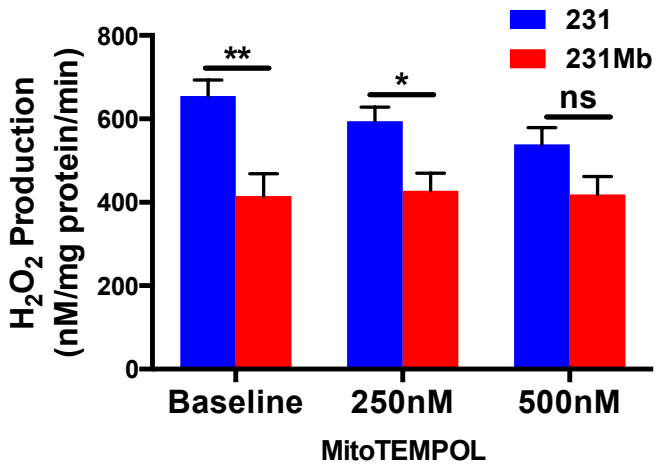

Figure 45. 231Mb cells do not produce mitochondrial ROS. As measured by the Amplex® Red assay and treating with mitoTEMPOLto scavenge mitochondrially-produced ROS, ROS production is not reduced in 231Mb cells. (** $p<0.001$, * $p<0.01$)

4.2.15 Myoglobin expression causes parkin oxidation in 231Mb cells

Because 231Mb cells produce a significant amount of cytosolic ROS, this ROS could oxidize parkin. Oxidized parkin is unable to mediate ubiquitination of mfns, thus resulting in excessive mitochondrial fusion Parkin oxidation was measured by a modified biotin switch assay in which parkin in pulled down by immunoprecipitation and oxidized residues labeled with biotin. Biotin levels are then normalized to the amount of parkin in the cell. As shown in Figure 46, these results revealed parkin oxidation is significantly greater in 231Mb cells.

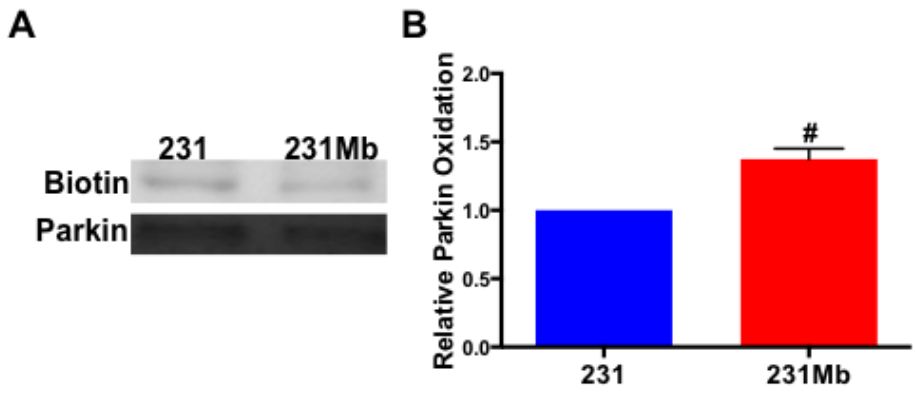

Figure 46. Parkin oxidation is significantly increased in 231Mb cells. Biotin levels are normalized to parkin levels in the cell. Data are presented as mean ± SEM. (# $p<0.05$)

5.0 DISCUSSION

Although myoglobin was first discovered over 100 years ago and its 3-dimensional structure resolved by X-ray crystallography over 50 years ago, new functions and locations of myoglobin are still being discovered today. As several groups have shown, myoglobin is expressed in tissues besides skeletal muscle including cancer tumors of non-muscle origin and has functions beyond oxygen storage and transport [22]. Specifically, myoglobin is able to scavenge or generate nitric oxide depending on oxygen tension in the cell [21]. As demonstrated in this thesis, these novel functions of myoglobin are important in mitochondrial regulation, particularly in ischemia/reperfusion injury and breast cancer.

The ubiquitously expressed anion nitrite is known to be protective against ischemia/reperfusion injury [ref]. In 2013, Chouchani et al. demonstrated that this protection occurs through S-nitrosation of the ND3 subunit of complex I, causing inactivation of complex I, which inhibits ROS production during reperfusion [47]. Here, the mechanism by which nitrite is reduced to nitric oxide to mediate complex I protection to promote cell survival was investigated.

Utilizing CHOR cells not expressing myoglobin and stably transfecting them to generate myoglobin-expressing CHOMb cells, it was shown by simulating ischemia/reperfusion *in vitro* that myoglobin is necessary for nitrite to mediate protection after ischemia/reperfusion (Figure 16). Moreover, by knocking down complex I of the electron transport chain in CHOR and CHOMb cells, it was shown that this protection occurs through complex I (Figure 19). It was also verified that the nitrite-mediated complex I protection occurs though S-nitrosation (Figure 17).

With this insight into the mechanism by which myoglobin and nitrite mediate protection in ischemia/reperfusion injury, nitrite treatment can be better targeted to cell types expressing myoglobin and nitrite dosing can be better tailored to meet a specific tissue's myoglobin content. Ischemia/reperfusion occurs in several pathological contexts including myocardial infarction, stroke, and organ transplantation. With the understanding of how nitrite reacts with myoglobin to reduce cell death and tissue damage, nitrite could be used to treat ischemia/reperfusion of other tissues. For example, during organ transplantation, the transplanted organ undergoes relatively a relatively long period of ischemia before reperfusion. However, it has been recognized that much of the tissue damage occurs during reperfusion injury. This injury to the tissue can result in delayed graft function as well as acute or chronic rejection [52]. With the emerging evidence that myoglobin is expressed in several tissues beyond skeletal muscle, some transplanted tissues may contain myoglobin, which would then allow for nitrite treatment to be utilized to reduce tissue damage during the reperfusion period after transplantation. In tissues that do not contain myoglobin, protein therapy may be utilized to force expression of myoglobin in order to allow nitrite treatment to be used to prevent tissue damage. Protein therapy, an emerging technology that is currently being investigated in several clinical trials, delivers a therapeutic level of a

protein to cells. There are several ways in which proteins can be delivered to the cell including PEGylation, nanoparticles, hyperglycosylation, and liposomes [53]. By forcing expression of myoglobin and treating with nitrite, during the ischemic period would cause respiration to be inhibited, thereby reducing cell death at the onset of reperfusion and ultimately preserving organ function.

While myoglobin has been shown to be protective by reducing cell death in ischemia/reperfusion, it has also emerged as a protective mechanism in cancer [22-24]. Investigation into myoglobin expression in breast cancer by Kristiansen and colleagues revealed that myoglobin expression is associated with better patient outcomes [22]. However, the role myoglobin plays in these tissues is not yet understood. By developing breast cancer cells that stably express human myoglobin, aim 2 of this thesis investigated how myoglobin affects cell proliferation and mitochondrial dynamics. Stably transfecting 231 breast cancer cells with human myoglobin (231Mb) revealed that myoglobin significantly reduces the proliferation of these cells (Figure 24). The effect of myoglobin expression on mitochondria was investigated by first examining overall mitochondria morphology. These results revealed that myoglobin-expressing cells have significant mitochondrial fusion while 231 control cells have very fragmented, punctate mitochondria (Figure 27 & Figure 28).

Interestingly, it has been shown by several groups that mitochondrial dynamics regulate the cell cycle. Specifically, proliferating cells have fragmented mitochondria whereas cell progressing from the G1 to S phase of the cell cycle have elongated, fused mitochondria. Mitochondrial hyperfusion can also occur at the G1/S transition, causing cell cycle arrest [48, 49]. Therefore, 231 cells have the mitochondrial phenotype of proliferating cells and 231Mb cells have a hyperfused phenotype and may be experiencing cell cycle arrest. Analysis of

expression of cyclin E and p21 expression, mediators of cell cycle progression at the G1/S transition, revealed that 231Mb cells have lower cyclin E and greater p21 expression than 231 control cells (Figure 34). Because cyclin E is required for cells to enter S phase of the cell cycle and p21 inhibits progression into S phase, these results suggest 231Mb cells experience cell cycle arrest at the G1/S phase transition.

Investigation into how myoglobin causes mitochondrial fusion, expression of the E3 ubiquitin ligase protein parkin was analyzed. Parkin, which facilitates ubiquitination of mitofusin proteins, was found to be expressed at lower levels in 231Mb cells than 231 control cells (Figure 40). Thus, in 231Mb cells, mitofusins are ubiquitinated to a lesser extent, thereby causing mitochondrial hyperfusion to reduce cell proliferation.

Myoglobin expression in cancer is particularly interesting because its expression in these cells, which typically grow and divide extremely rapidly, causes a reduction in cell proliferation, thereby serving as a protective mechanism. This insight into how myoglobin may be a mediator of cell proliferation could be employed in several applications. For example, protein therapy could be utilized to reduce proliferation in cells that do not typically express myoglobin or have low myoglobin expression. This could be particularly interesting in smooth muscle cells, as rapid proliferation of smooth muscle cells becomes important in the progression of atherosclerosis. Although these cells have been shown to express myoglobin, it is only expressed in low levels [21]. Therefore, protein therapy could be used to force myoglobin expression and potentially inhibit smooth muscle cell proliferation to slow disease progression.

It would also be interesting to investigate whether myoglobin is expressed in various stages of development. Through development, cells go through stages in which they proliferate very rapidly and many eventually stop regenerating completely. For proper development,

proliferation of each cell type needs to be coordinated and very tightly regulated. It would be interesting to investigate whether myoglobin expression is one way in which these cells transform from rapidly proliferating to terminally differentiated cells.

Myoglobin expression in cancer also poses a novel therapeutic target for treatment. In 2008, Wittenberg suggested non-toxic concentrations of carbon monoxide could be used to target myoglobin in these tumors [22]. Myoglobin expression could also be used to classify breast cancer cases in order to provide better treatment options and better understand the progression of the disease for individual patients. In breast cancer patients with myoglobin negative tumors, myoglobin could be used as protein therapy to reduce proliferation and spread of the cancer. Although this is not a treatment for cancer, it could aid in significantly reduce tumor growth, which would allow the cancer to be treated more effectively.

In summary, myoglobin and mitochondria have long been known to be critical for normal cell function; however, they have only recently been recognized to interact. Here, it is shown that myoglobin is necessary to reduce nitrite to nitric oxide for protection against cell death after ischemia/reperfusion injury, thereby promoting cell survival. Additionally, it is shown that myoglobin functions as a protective mechanism in breast cancer, modulating mitochondrial dynamics to reduce cell proliferation and tumor growth. It is clear that myoglobin has a wide variety of functions and although it was once thought of only as an oxygen storage protein, it may play a role in more diseases than what is currently understood.

6.0 FUTURE DIRECTIONS

This project showed that nitrite is reduced to nitric oxide by myoglobin in hypoxia, which S-nitrosates complex I to reduce cell death in reperfusion. However, the method used verified this protection occurs through complex I by knocking down the entire complex, which may cause additional complications within the cell that may have other effects not obvious in this experiment. A better, more focused approach would be to mutate the cysteine 39 on the ND3 subunit of complex I, which is the residue Chouchani et al. found to be modified after nitrite treatment in ischemia/reperfusion [47]. In this case, other effects of knocking down complex I would be eliminated and it would be further validated that the protection occurs by S-nitrosation of this residue. Unfortunately, however, this method cannot be utilized. The complexes of the electron transport chain are encoded by mitochondrial DNA. Although much research has been invested into studying the mitochondrial genome, to date a method to modify the DNA has not yet been developed [54].

An alternative would be to measure the activity of all complexes of the electron transport chain in CHOR and CHOMb cells with and without nitrite treatment after ischemia/reperfusion simulation. With nitrite treatment, the activity of complex I in CHOMb cells should be significantly reduced, since nitrite S-nitrosates the ND3 subunit to inhibit complex I and mediate protection. In the CHOR cells, complex I activity should not be inhibited significantly, as electrons will continue to enter the chain at this complex, which will leak out, eventually

resulting in ROS production (Figure 11). Additionally, it would be useful to measure ROS production in the CHOR and CHOMb cells after ischemia/reperfusion to determine how much nitrite reduces ROS production in CHOMb cells.

While the results presented in this thesis suggest myoglobin may significantly reduce breast cancer cell proliferation, further research is warranted. It is important to study the effect of myoglobin expression on other cancer cell types. The MDA-MB-231 cell line is triple negative cell line, meaning it does not have receptors for estrogen (ER), progesterone (PR), or HER-2/neu. However, only between 10 and 17% of breast cancers are triple negative while 65% are PR positive and 75% ER positive [55]. Therefore, for this research to be most clinically relevant, it is important to understand how myoglobin's effects differ based on hormone receptor status. Specifically, the MCF-7 cell line, which is ER and PR positive, could be used to study the effect of positive hormone receptor status. Further, because some patients have highly metastatic breast cancer while others do not experience metastasis, it would also be beneficial to study cell lines with different metastatic ability. The cell line MDA-MB-468 could be used to determine whether myoglobin expression has different effects depending on the metastatic ability of the cells. The MDA-MB-468 cell line is also triple negative; therefore by comparing these results to the proliferation results of MDA-MB-231 cells, myoglobin's effect on cells of different metastatic ability could be investigated independent of hormone receptor status. Another important avenue to explore is the effect of myoglobin expression on premalignant human breast epithelial cells. To investigate whether myoglobin has the same antiproliferative effect on cells before they are considered cancerous, MCF-10A cells, which are normal breast epithelial cells, could be transfected with myoglobin. This would provide insight into when myoglobin may begin to be expressed in breast cancer, before or after the cell becomes tumorigenic.

The results presented in this thesis suggest myoglobin may act as a tumor suppressor by reducing breast cancer cell proliferation. It is important to test whether this phenomenon occurs in other cell types, including other types of cancer. Preliminary results from Galluzzo et al. in 2009 suggest myoglobin expression in lung cancer cells also reduces proliferation and delays tumor engraftment *in-vivo* [56]. Therefore, the effect of forced myoglobin expression should be investigated in several cancer cell types including lung, colon, and ovary, because it has been reported that these tumor types show myoglobin expression *in vivo*. It is also important to investigate whether myoglobin's ability to reduce cell proliferation is translatable to other non-cancerous cell types. Preliminary results from our lab suggest myoglobin expression in the CHO cell line does not have the same effect on proliferation as in the MDA-MB-231 cells. Therefore, this phenomenon of myoglobin reducing cell proliferation may be unique to cancer cells, which could provide significant advancements in the treatment of cancer and understanding of its progression.

Additionally, although the preliminary results presented here suggest myoglobin reduces tumor growth *in vivo*, it is necessary to perform further animal experiments. For example, other injection methods could be utilized. In this project, 3×10^6 cells were injected into the mammary fat pad of the mice, which can result in significant cell death and few cells are actually implanted and contribute to tumor formation. Alternatively, a subcutaneous injection method could be used. Several other aspects of tumor growth should also be investigated including metastatic spread to foreign tissues and angiogenesis at the site of the tumor. Because it was found that 231Mb cells migrate significantly less than 231 control cells, metastasis would be interesting to investigate, as breast cancer is known to metastasize to several tissues, specifically the lungs, brain, bone, and liver. By injecting mice with breast cancer cells through tail vein injection, metastasis to the lungs can be studied.

The recent discovery of myoglobin in smooth muscle cells poses additional therapeutic uses for myoglobin. In atherosclerosis, and restenosis after stent placement, rapid proliferation of vascular smooth muscle cells contributes to progression of these disorders. Although these cells contain low levels of endogenous myoglobin, if myoglobin's ability to reduce cell proliferation is translatable to smooth muscle cells, forcing myoglobin expression in these cells may be a means by which the progression of these disorders could be slowed. Moreover, it would be advantageous to examine whether the level of myoglobin expression changes as restenosis and atherosclerosis progress. This would provide insight into whether there is a molecular switch within the cells, causing them to proliferate excessively, and whether myoglobin contributes to this change in phenotype.

7.0 CONCLUSIONS

This research confirms that myoglobin has several functions in addition to oxygen storage and delivery in skeletal muscle. Myoglobin was found to be essential for nitrite-mediated protection in ischemia/reperfusion injury through post-translational modification of complex I, which promotes cell survival and mitigates tissue damage. Moreover, myoglobin was shown to function as a protective mechanism to reduce cell proliferation in breast cancer both *in vitro* and *in vivo* through modulation of mitochondrial dynamics and function. This may contribute to improving patient prognosis in those patients with myoglobin-expressing tumors.

With these insights into how myoglobin modulates mitochondria, better understanding of disease progression can be established, which will allow for development of improved treatment methods. Moreover, with further research, the expression profile of myoglobin will continue to be clarified, which may allow for nitrite-based therapies to be utilized in additional applications such as organ transplantation. In conclusion, myoglobin is a protein with several functions that are still being elucidated today and has the potential to be employed in treatment of disease and used to better understand disease progression.

BIBLIOGRAPHY

1. Mitchell P, *Coupling of phosphorylation to electron and hydrogen transfer by a chemi-osmotic type of mechanism*. Nature. 1961. 191(4784): p. 144-148.

2. Haynie DT. *Biological Thermodynamics*. New York: Cambridge University Press, 2008.

3. Nelson DL, Lehninger AL, Cox MM. *Lehninger Principles of Biochemistry.* New York: W.H. Freeman and Company, 2008.

4. Murphy MP. *How mitochondria produce reactive oxygen species.* Biochemical Journal. 2009. 417: p. 1-13.

5. Kamga Pride C, Mo L, Quesnelle K, Dagda RK, Murillo D, Geary L, Corey C, Portella R, Zharikov S, St Croix C, Maniar S, Chu CT, Khoo NKH, Shiva S. *Nitrite activates protein kinase A in normoxia to mediate mitochondrial fusion and tolerance to ischemia/reperfusion.* Cardiovascular Research. 2014. 101(1): p. 57-68.

6. Ray PD, Huang BW, Tsuji Y. *Reactive oxygen species (ROS) homeostasis and redox regulation in cellular signaling*. Cellular Signaling. 2012. 24(5): p. 981-90.

7. Kvansakul M and Hinds MC. *The Bcl-2 family: structures, interactions and targets for drug discovery*. Apoptosis. 2015. 20(2): p. 135-50.

8. Youle RJ, and Bliek AM, *Mitochondrial Fission, Fusion, and Stress*. Science. 2012. 337(6098): p. 1062-65.

9. Knott AB, Perkins G, Schwartzenbacher R, Bossy-Wetzel E. *Mitochondrial fragmentation in neurodegeneration*. Nature Reviews Neuroscience. 2012. 9(7): p. 505-518.

10. Rossignol R, Gilkerson R, Aggeler R, Yamagata K, Remington SJ, Capaldi RA. *Energy substrate modulates mitochondrial structure and oxidative capacity in cancer cells.* Cancer Research. 2004. 64(3): p. 985-993.

11. Mörner KAH. Beobachtungen über den Muskelfarbstoff. Nord. Med. Ark. 1897. 30:1–8.

12. Günther, H. Über den Muskelfarbstoff. Virchows Arch. 1921. 230: p. 146-178.

13. Hendgen-Cotta UB, Flögel U, Kelm M, Rassaf T. *Unmasking the Janus face of myoglobin in health and disease.* Journal of Experimental Biology. 2010. 213: p. 2734-40.

14. Kendrew JC, Bodo G, Dintzis HM, Parrish RG, Wyckoff H, Phillips DC. *A Three-Dimensional Model of the Myoglobin Molecule Obtained by X-Ray Analysis*. Nature. 1958. 181(4610): p. 662–6.

15. Kendrew JC. *The three-dimensional structure of a protein molecule.* Scientific American. 1961. 205: p. 96-110.

16. Kamga C, Krishnamurthy S, Shiva S. *Myoglobin and mitochondria: A relationship bound by oxygen and nitric oxide*. Nitric Oxide. 2012. 26(4): 251-8.

17. Ordway GA and Garry DJ. *Myoglobin: an essential hemoprotein in striated muscle.* The Journal of Experimental Biology. 2004. 207: p. 3441-6.

18. Wittenberg BA and Wittenberg JB. *Transport of oxygen in muscle.* Annual Reviews of Physiology. 1989. 51: p. 857-78.

19. Springer BA, Egeberg KD, Sligar SG. *Discrimination between oxygen and carbon monoxide and inhibition of autooxidation by myoglobin. Site-directed mutagenesis of the distal histidine*. Journal of Biological Chemistry, 1989. 264(6): p. 3057-60.

20. Qiu Y, Sutton L, Riggs AF. *Identification of myoglobin in human smooth muscle.* Journal of Biological Chemistry. 1998. 273(36): p. 23426-32.

21. Totzeck M, Hendgen-Cotta UB, Luedike P, Berenbrink M, Klare JP, Steinhoff HJ, Semmler D, Shiva S, Williams D, Kipar A, Gladwin MT, Schrader J, Kelm M, Cossins AR, Rassaf T. *Nitrite regulates hypoxic vasodilation via myoglobin–dependent nitric oxide generation*. Circulation. 2012. 126(3): p. 325-34.

22. Kristiansen G, Rose M, Geisler C, Fritzsche FR, Gerhardt J, Lüke C, Ladhoff AM, Knüchel R, Dietel M, Moch H, Varga Z, Theurillat JP, Gorr TA, Dahl E. *Endogenous myoglobin in human breast cancer is a hallmark of luminal cancer phenotype.* British Journal of Cancer. 2010. 102(12): p. 1736-45.

23. Galluzzo M, Pennacchietti S, Rosano S, Cornoglio PM, Michielo P, *Prevention of hypoxia by myoglobin expression in human tumor cells promotes differentiation and inhibits metastasis*. Journal of Clinical Investigation. 2009. 119(4): p. 865-75.

24. Flonta S.E., Arena S, Pisacane A, Michieli P, Bardelli, A, *Expression and functional regulation of myoglobin in epithelial cancers.* American Journal of Pathology. 2009. 175(1): p. 201-206.

25. Wittenberg JB and Wittenberg BA. *Myoglobin function reassessed.* Journal of Experimental Biology. 2003. 206: p. 2011-20.

26. Molé PA, Chung Y, Tran TK, Sailasuta N, Hurd R, Jue T. *Myoglobin desaturation with exercise intensity in human gastrocnemius muscle*. American Journal of Physiology. 1999. 277: p. R173-80.

27. Wittenberg JB. *Myoglobin-facilitated oxygen diffusion: role of myoglobin in oxygen entry into muscle*. Physiology Reviews. 1970. 50(4): p. 559-636.

28. Wittenberg BA and Wittenberg JB, *Myoglobin-mediated oxygen delivery to mitochondria of isolated cardiac myocytes,* PNAS. 1987. 84(21): p. 7503-07.

29. Lin PC, Kreutzer U, Jue T. *Myoglobin translational diffusion in rat myocardium and its implication on intracellular oxygen transport*. Journal of Physiology. 2007. 578: p 595-603.

30. Johnson RL, Heigenhauser GJF, Hsia CCW, Jones NL, Wagner PD. *Determinants of Gas Exchange and Acid–Base Balance During Exercise*. Comprehensive Physiology. 2011. p. 515–584.

31. Takahashi E, H Endoh, Doi K. *visualization of myoglobin-facilitated mitochondrial O2 delivery in a single isolated cardiomyocyte*. Biophysical Journal. 2000. 78(6): p. 3252-59.

32. Merx MW. Flögel U, Stumpe T, Gödecke A, Decking U, Schrader J. *Myoglobin facilitates oxygen diffusion*. The FASEB Journal. 2001. 78(6): p. 3252-9

33. Cosby K, Partovi KS, Crawford JH, Patel RP, Reiter CD, Martyr S, Yang BK, Waclawiw MA, Zalos G, Xu X, Huang KT, Shields H, Kim-Shapiro DB, Schechter AN, Cannon RO, Gladwin MT. *Nitrite reduction to nitric oxide by deoxyhemoglobin vasodilates the human circulation.* Nature Medicine. 2003. 9(12): p. 1498-505.

34. Gladwin MT and Kim-Shapiro DB, *The functional nitrite reductase activity of the heme-globins*. Blood. 2008. 112(7): p. 2636-47.

35. Huang Z, Shiva S, Kim-Shapiro DB, Patel RP, Ringwood LA, Irby CE, Huang KT, Ho C, Hogg N, Schechter AN, Gladwin MT. *Enzymatic function of hemoglobin as a nitrite reductase that produces no under allosteric control*. Journal of Clinical Investigation. 2005.115(8): p. 2099-2107.

36. Brunori M. *Nitric oxide, cytochrome-c oxidase and myoglobin*. Trends in Biochemical Sciences. 2001. 26(1): p. 21-3.

37. Brunori M. *Myoglobin Strikes Back*. Protein Science. 2010. 19(2): p. 195-201.

38. Shiva S, Brookes PS, Patel RP, Anderson PG, Darley-Usmar VM. *Nitric oxide partitioning into mitochondrial membranes and the control of respiration at cytochrome c oxidase*. PNAS. 2001. 98(13): p. 7212-17.

39. Thomas DD, Liu X, Kantrow SP, Lancaster JR. *The biological lifetime of nitric oxide: implications for the perivascular dynamics of NO and O2*. PNAS. 2001. 98(1): p. 355-60.

40. Brookes PS, Kraus DW, Shiva S, Doeller JE, Barone MC, Patel RP, Lancaster JR, Darley-Usmar V. *Control of mitochondrial respiration by NO*, effects of low oxygen and respiratory state*. Journal of Biological Chemistry. 2003. 278(34): p. 1603-9.

41. Brown GC. *Regulation of mitochondrial respiration by nitric oxide inhibition of cytochrome c oxidase.* Biochimica et Biophysica Acta. 2001. 1504(1): p. 46-57.

42. Shiva A, Sack MN, Greer JJ, Duranski M, Ringwood LA, Burwell L, Wang X, MacArthur PH, Shoia A, Raghavachari N, Calvert JW, Brookes PS, Lefer DJ, Gladwin MT. *Nitrite augments tolerance to ischemia/reperfusion injury via the modulation of mitochondrial electron transfer*. Journal of Experimental Medicine. 2007. 204(9): p: 2089-102.

43. Hendgen-Cotta UB, Merx MW, Shiva S, Schmitz J, Becher S, Klare JP, Steinhoff HJ, Goedecke A, Schrader J, Gladwin MT, Kelm M, Rassaf T. *Nitrite reductase activity of myoglobin regulates respiration and cellular viability in myocardial ischemia-reperfusion injury*. PNAS. 2008. 105(29): p. 10256-61.

44. Schlieper G, Kim JH, Molojavyi A, Jacoby C, Laussmann T, Flögel U, Gödecke A, Schrader J. *Adaptation of the myoglobin knockout mouse to hypoxic stress*. American Journal of Physiology. 2003. 286(4).

45. Honda HM, Korge P, Weiss JN. *Mitochondria and ischemia/reperfusion injury*. Annals of the New York Academy of Science. 2005. 1047: p. 248-58.

46. Jassem W and Heaton ND. *The role of mitochondria in ischemia/reperfusion injury in organ transplantation*. Kidney International. 2004. 66(2): p. 514-17.

47. Chouchani ET, Methner C, Nadtochiy SM, Logan A, Pell VR, Ding S, James AM, Cochemé HM, Reinhold J, Lilley KS, Partridge L, Fearnley IM, Robinson AJ, Hartley RC, Smith RAJ, Krieg T, Brookes PS, Murphy MP. *Cardioprotection by S-nitrosation of a cysteine switch on mitochondrial complex I*. Nature Medicine. 2013. 19(6): p. 753-59.

48. Mitra K, Wunder C, Roysam B, Lin G, Lippincott-Schwartz J. *A hyperfused mitochondrial state achieved at G1–S regulates cyclin E buildup and entry into S phase*. PNAS. 2009. 106(29): p. 11960-5.

49. Yamano K and Youle RJ. *Coupling mitochondrial and cell division.* Nature Cell Biology. 2011. 13(9): p. 1026-27.

50. Lim KL, Ng XH, Grace LGY, Yao TP. *Mitochondrial dynamics and parkinson's disease: focus on parkin*. Antioxidants and Redox Signaling. 2012. 16(9): p. 935-49.

51. Metzger MB, Pruneda JN, Klevit RE, Weissman AM. *RING-type E3 ligases: Master manipulators of E2 ubiquitinconjugating enzymes and ubiquitination*. Biochimica et Biophysica Acta. 2014. 1843(1): p. 47-60.

52. Cicco G, Panzera PC, Catalano G, Memeo V. *Microcirculation and reperfusion Injury in organ transplantation*. Advances in Experimental Medicine and Biology. 2005. 566: p. 363-73.

53. Pisal DS, Kosloski MP, Balu-lyer SV. *Delivery of Therapeutic Proteins.* Journal of Pharmaceutical Science. 2011. 99(6): p. 2557-75.

54. Yoon YG, Koob MD, Yoo YH. *Re-engineering the mitochondrial genomes in mammalian cells.* Anatomy and Cell Biology. 2010. 43(2): p. 97-109.

55. Types of Breast Cancer: Triple Negative, ER Positive, HER2 Positive. (n.d.). http://www.webmd.com/breast-cancer/breast-cancer-types-er-positive-her2-positive

56. Galluzzo M, Pennacchietti S, Rosano S, Cornoglio PM, Michielo P, *Prevention of hypoxia by myoglobin expression in human tumor cells promotes differentiation and inhibits metastasis.* Journal of Clinical Investigation. 2009. 199(4): p. 865-75.